Molecular Capacitors: Accessible 6- and 8-electron Redox Chemistry from Dimeric "Ti(I)" and "Ti(0)" Synthons Supported by Imidazolin-2-Iminato Ligands.

Alejandra Gómez-Torres,[a] Niki Mavragani,[b] Alejandro Metta-Magaña,[a] Muralee Murugesu,[b] and Skye Fortier[a,*]

[a]Department of Chemistry and Biochemistry, University of Texas at El Paso, El Paso, Texas 79968
[b]Department of Chemistry and Biomolecular Sciences, University of Ottawa, Ottawa, Ontario K1N 6N5

ABSTRACT: Reduction of the diamagnetic Ti(III)/Ti(III) dimer $[Cl_2Ti(\mu\text{-}NIm^{Dipp})]_2$ (**1**) (NIm^{Dipp} = [1,3-bis(Dipp)imidazolin-2-iminato]$^-$, Dipp = NC_6H_3-2,6-Pr^i_2) with 4 and 6 equiv of KC_8 generates the intramolecularly arene-masked, dinuclear titanium compounds $[(\mu\text{-}N\text{-}\mu\text{-}\eta^6\text{-}Im^{Dipp})Ti]_2$ (**2**) and $\{[(Et_2O)_2K](\mu\text{-}N\text{-}\mu\text{-}\eta^6\text{:}\eta^6\text{-}Im^{Dipp})Ti\}_2$ (**3**), respectively, in modest yields. The compounds have been structurally characterized by X-ray crystallographic analysis and inspection of the bond metrics within the η^6-coordinated aryl substituent of the bridging imidazolin-2-iminato ligand show perturbation of the aromatic system most consistent with two-electron reduction of the ring. As such, **2** and **3** can be assigned respectively as possessing metal centers in formal Ti(III)/Ti(III) and Ti(II)/Ti(II) oxidation states. Exploration of their redox chemistry reveal the ability to reduce several substrate equivalents. For instance, treatment of **2** with excess C_8H_8 (COT) forms the novel COT-bridged complex $[(Im^{Dipp}N)(\eta^8\text{-COT})Ti](\mu\text{-}\eta^2\text{:}\eta^3\text{-COT})[Ti(\eta^4\text{-COT})(NIm^{Dipp})]$ (**4**) that dissociates in THF solutions to give mononuclear $(Im^{Dipp}N)Ti(\eta^8\text{-COT})(THF)$ (**5**). Addition of COT to **3** yields heterometallic $[(Im^{Dipp}N)(\eta^4\text{-COT})Ti(\mu\text{-}\eta^4\text{:}\eta^5\text{-COT})K(THF)(\mu\text{-}\eta^6\text{:}\eta^4\text{-COT})Ti(NIm^{Dipp})(\mu\text{-}\eta^4\text{:}\eta^4\text{-COT})K(THF)_2]_n$ (**6**). Compounds **2** and **5** are the products of the 4-electron oxidation of **2**, while **6** stands as the 8-electron oxidation product of **3**. Reduction of organozides was also explored. Low temperature reaction of **2** with 4 equiv of AdN_3 gives the terminal and bridged imido complex $[(Im^{Dipp}N)Ti(=NAd)](\mu\text{-}NAd)_2[Ti(NIm^{Dipp})(N_3Ad)]$ (**7**) that undergoes intermolecular C-H activation of toluene at room temperature to afford the amido compound $[(Im^{Dipp}N)Ti(NHAd)](\mu\text{-}NAd)_2[Ti(C_6H_4Me)(NIm^{Dipp})]$ (**8-tol**). These complexes are the 6-electron oxidation products of the reaction of **2** with AdN_3. Furthermore, treatment of **3** with 4 equiv of AdN_3 produces the thermally stable Ti(III)/Ti(III) terminal and bridged imido $[K(18\text{-crown-}6)(THF)_2]\{[(Im^{Dipp}N)Ti(NAd)](\mu\text{-}NAd)_2K[Ti(NIm^{Dipp})]\}$ (**10**). Altogether, these reactions firmly establish **2** and **3** as unprecedented Ti(I)/Ti(I) and Ti(0)/Ti(0) synthons with the clear capacity to effect multi-electron reductions ranging from 4 – 8 electrons.

INTRODUCTION

Discrete molecular compounds capable of achieving multi-electron transfers, outside of molecular electrochemical catalysts, are important for modeling the electron transfer chemistry of enzymatic systems,[1-2] enabling new charge transport layers in solar devices[3] and anodic materials for batteries,[4] while also effecting such biologically relevant transformations as O_2 and CO_2 reduction.[5-7] Extended aromatic π-systems such as fullerenes are competent charge carriers C_{60}^{n-} (n = 0 – 6)[8-9] but are limited in their ability to accomplish the chemical transformation of small molecules. With regards to this latter aspect, multi-metallic systems have demonstrated most promise.

In principle, polynuclear clusters, LM_n (n > 2), are ideal candidates for enabling the reduction of small molecules as the chemistry is facilitated by redox cooperativity, namely distributing multielectron transfers across several metal centers. Additionally, each metal may offer a binding site that provides separate reaction centers allowing for the synergistic activation of small molecule substrates.[7, 10-11] For instance, nitrogenase features a Fe_7MoS_9C active site that mediates the 6-electron reduction of N_2, and work by Hoffman and co-workers implicates involvement of several of the iron atoms in the intermediate steps of the reaction.[10]

Building upon this idea, the Betley group has shown that the trinuclear iron compound $(^{tbs}L)Fe_3(THF)$ ($[^{tbs}L$ = [1,3,5-$C_6H_9(NC_6H_4$-*o*-$NSi^tBuMe_2)_3]^{6-}$) performs 2 and 4-electron reduction of hydrazines and azobenzene, respectively, to generate $(^{tbs}L)Fe_3(\mu_3\text{-}NH)$ and $(^{tbs}L)Fe_3(\mu_3\text{-}NPh)(\mu_2\text{-}NPh)$.[1] Electrochemical study supports a cooperative electron transfer mechanism in the hydrazine and diazene activation. Mazzanti and co-workers have combined hexanuclear iron assemblies with redox active salophen ligands in $Na_{12}Fe_6$(tris-cyclo-salophen)$_2(THF)_{14}$ that synergistically reduce CO_2 with selective formation of carbonate.[6] Using β-diketiminate functionalized cyclophane ligands, Murray and co-workers have elegantly demonstrated multielectron transfer and cooperative reactivity in their trimetallic clusters.[7] Treatment of (cyclophane)Co_3 (cyclophane = $\{(C_6Et_3CH_2)_2[(N)CCH_3CH_3C(N)]_3\}^{3-}$), possessing a metal-metal bonded core, with N_2 leads to scission of the metallic bonds and formation of (cyclophane)$Co_3(N_2)$ with reduction of the dinitrogen bond order, where adding Me_3SiBr produces $N(SiMe_3)_3$ in good yield.[12] With respect to the earlier 3d metals, Matson et al. have demonstrated the successful implementation of a vanadium polyoxometalate cluster for the reduction of O_2 to H_2O.[5] Reduction of $[V_6O_{13}(TRIOL^{NO2})_2]^{2-}$ ($TRIOL^{NO2}$ = $[(OCH_2)_3C(NO_2)]^{3-}$) by 6-electron and proton equivalents yields $[V_6O_7(OH)_6(TRIOL^{NO2})_2]^{2-}$, where the latter product reacts with excess O_2 to produce 3 equiv. of H_2O. Notably, in all these cases, the reduced species are isolable and clearly carry a capacitance for multielectron transfer.

Alternatively, multiply bonded metal-metal complexes have been shown capable of storing high charge capacity within their metallic bonds. Quintuply bonded dichromium and dimolybdenum complexes have been demonstrated to readily undergo 2, 4, 6, and even 8-electron oxidations.[13] Power's Ar'_2Cr_2 (Ar' = C_6H_3-2,6-$(C_6H_3$-2,6-$^iPr_2)_2]^-$) reacts with excess N_2O to produce $Ar'Cr(\mu\text{-}O)_2Cr(O)Ar'$ via 6-electron oxidation,[14] releasing N_2 as the byproduct. Moreover, exposure of Kempe, Kaupp, and co-workers' L'_2Cr_2 (L' = $[(C_6H_3{}^iPr_2)NC_5H_3(NC_6H_3Me_2)]^-$) to molecular oxygen results in the formation of the doubly terminal and oxo bridged complex $[L'_2Cr(O)(\mu\text{-}O)]_2$, via formal 8-electron oxidation distributed over the two chromium centers.[15]

In recent years, impressive strides have been made in the development of the low-valent chemistry of the early metals

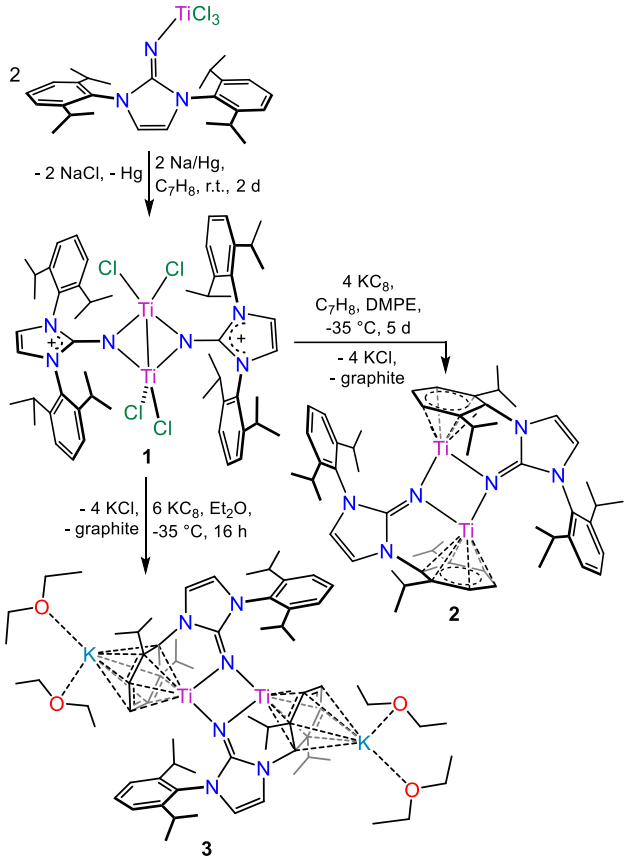

Scheme 1. Synthesis of **1**, **2**, and **3**.

(electron counts ≥d^2), showing these systems to be formidable reductants capable of small molecule activation that can also mediate important organic chemistries.[16-19] In our own laboratory, we have shown that the reduced arene-masked titanium complexes (^{Arket}guan)Ti(η^6-NIm^{Dipp}) (^{Arket}guan = [(^{t}Bu$_2$CN)C(NAr)$_2$]$^-$, Ar = C$_6$H$_3$-2,6-^{i}Pr$_2$ (**A**), C$_6$H$_3$-3,5-Me$_2$ (**B**); Im^{Dipp}N = [1,3-bis(Dipp)imidazolin-2-iminato]$^-$, Dipp = NC$_6$H$_3$-2,6-^{i}Pr$_2$) can perform the catalytic hydrogenation of mono- and polycyclic aromatic hydrocarbons as well as accomplish the hydrodesulfurization (HDS) of thiophene.[20-22] The latter example is particularly noteworthy as the titanium complex shows a very rare display of fully reversible, early-metal oxidative-addition/reductive-elimination during the initial HDS step involving ring opening of the thiophene. Nevertheless, these chemistries are limited to two-electron redox cycling.

Highly reduced multi-metallic assemblies containing early-metals that can promote redox transformations involving 4 or more electrons are few in number. Cloke et al. have shown that the Ti=Ti pentalene sandwich complex (μ-η^5:η^5-Pn)$_2$Ti$_2$ (Pn = [1,4-(^{t}Pr$_3$Si)$_2$C$_8$H$_4$]$^{2-}$) reacts with a host of small molecules to perform 2 and 4-electron reductions.[19, 23-27] As an example, (μ-η^5:η^5-Pn)$_2$Ti$_2$ reacts with 1 equiv. of CO$_2$ to produce [(η^5:η^5-Pn)Ti]$_2$(μ-O),[24] releasing an equiv. of CO, while the reaction with azobenzene provides [(η^5:η^5-Pn)Ti]$_2$(μ-NPh)$_2$.[25] Similarly, Arnold and coworkers have shown that the N$_2$-bridged complex {[PhC(NSiMe$_3$)$_2$]$_2$Ti}$_2$(μ-N$_2$) reduces O$_2$ to afford [κ^2-PhC(NSiMe$_3$)$_2$][κ^1-PhC(NSiMe$_3$)$_2$]Ti(μ-O)$_2$Ti[κ^2-PhC(NSiMe$_3$)$_2$]$_2$.[28] The titanium-hydride cluster {[(C$_5$Me$_4$SiMe$_3$)Ti]$_3$(μ$_3$-H)(μ$_2$-H)$_6$} reported by Zhou et al. cleaves N$_2$ to yield {[(C$_5$Me$_4$SiMe$_3$)Ti]$_3$(μ$_2$-NH)(μ$_3$-N)(μ$_2$-H)$_2$}. Yet, the reactive hydride cluster formally features high valent titanium (Ti(IV), Ti(III)), where the reducing equivalents are provided by the hydride ligands.[29]

The 2-electron redox chemistry observed in **A** and **B** is enabled by the unexpected redox non-innocence of the Im^{Dipp}N ligand. Leveraging this, we reasoned that paring the guanidinate ligand from these systems would favor the formation of highly reduced, multi-metallic early-metal compounds able to perform redox chemistry exceeding that observed for **A** and **B**. To this end, reduction of (Im^{Dipp}N)TiCl$_3$ with sodium amalgam produces the dinuclear Ti(III) complex [Cl$_2$Ti(μ-NIm^{Dipp})]$_2$ (**1**), which can be subsequently reduced to afford [(μ-N-μ-η^6-Im^{Dipp})Ti]$_2$ (**2**) and {[(Et$_2$O)$_2$K](μ-N-μ-η^6:η^6-Im^{Dipp})Ti}$_2$ (**3**). To the best of our knowledge, **2** and **3** are the first examples of discrete Ti(I)/Ti(I) and Ti(0)/Ti(0) synthons, respectively. In an initial examination of their reactivity profiles, **2** and **3** react with organoazides and cyclooctatetraene (COT) through a series of 4, 6, and 8-electron transfers, successfully demonstrating high charge storage in bimetallic early-metal complexes.

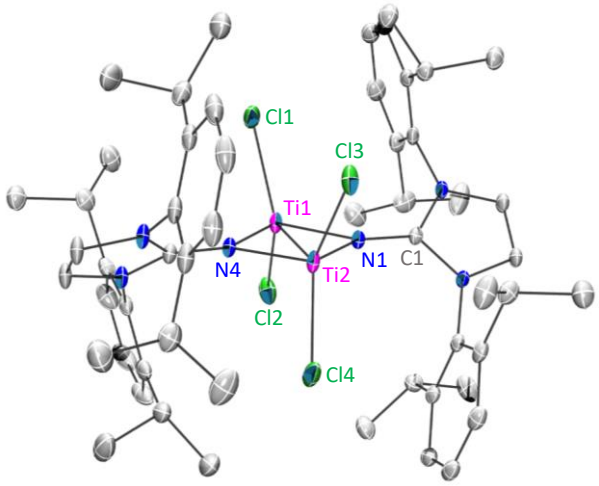

Figure 1. Solid-state molecular structure of **1**·1.5C$_7$H$_8$ with 30% probability ellipsoids. Hydrogen atoms and co-crystallized toluene molecules are omitted for clarity. Selected bond lengths (Å) and angles (deg): Ti1-Ti2 = 2.6183(6), Ti1-N1 = 1.972(2), Ti1-N4 = 1.974(2), Ti2-N1 = 1.963(2), Ti2-N4 = 1.974(2), N1-C1 = 1.327(3), N4-C28 = 1.322(3), Ti1-N1-Ti2 = 83.43(7), Ti1-N4-Ti2 = 83.09(7).

RESULTS AND DISCUSSION

Synthesis and Characterization of Reduced Titanium Dimers. Compound **1** is synthesized from the room temperature reduction of (Im^{Dipp}N)TiCl$_3$ with 2 equiv of Na/Hg in toluene over two days (Scheme 1). Diamond-shaped dark blue crystals of **1**·1.5C$_7$H$_8$ can be isolated in 79% yield from concentrated toluene solutions layered with pentane and stored at -35 °C for 12 h.

Complex **1**·1.5C$_7$H$_8$ crystallizes in the monoclinic space group *C*2/*c* with one full molecule in the asymmetric unit (Figure 1). The molecule consists of a dimer possessing terminal chlorides with bridging imidazolin-2-iminato ligands giving a Ti$_2$(μ-NIm^{Dipp})$_2$ diamond core. The Ti-N distances in **1**·1.5C$_7$H$_8$ range from 1.963(2) to 1.974(2) Å, which are similar to the Ti-N$_{imido}$ = 1.938(3) – 1.994(4) Å bond distances found in the imido-bridged Ti(III) dimer [(^{t}Bu$_3$SiNH)Ti(μ-NSi^{t}Bu$_3$)]$_2$.[30] This is interesting as the Im^{Dipp}N ligand is monoanionic, suggesting an ylidic zwitterionic resonance structure where the bridging *N*-atom adopts dianionic character. This is a common resonance form for imidazolin-2-iminato ligands,[31] and in line with this assessment, the N1-C1 = 1.327(3) Å and N4-C28 = 1.322(3) Å bond distances are significantly elongated as compared to the corresponding bond lengths found in the dimeric lithium salt [Li(μ-Nim^{Dipp})]$_2$ (N-C = 1.241(3) 1.242(4) Å).[32]

The Ti1-Ti2 bond length in **1**·1.5C$_7$H$_8$ is 2.6183(6) Å, which is longer than that found in [(^{t}Bu$_3$SiNH)Ti(μ-NSi^{t}Bu$_3$)]$_2$ (Ti-Ti =

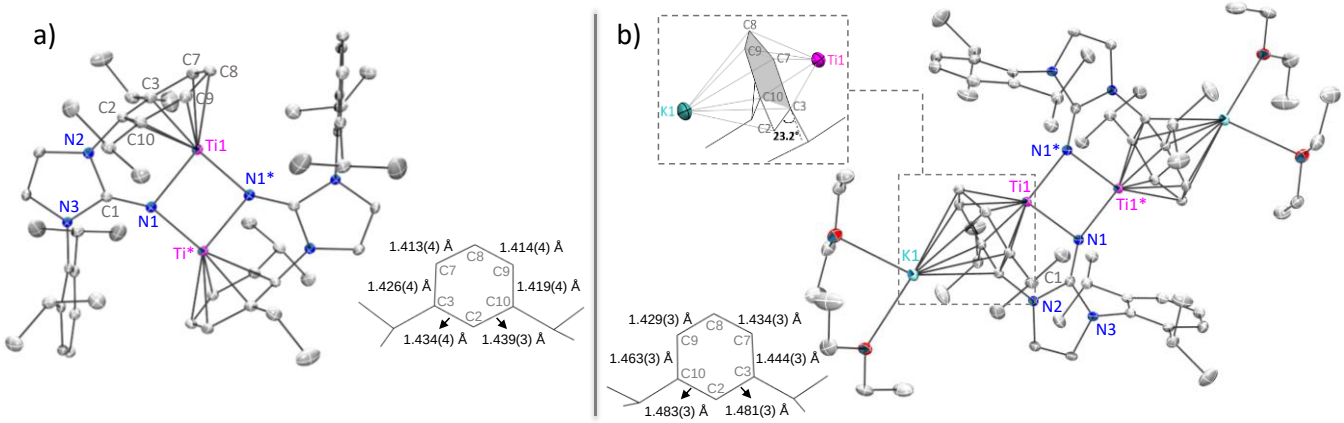

Figure 2. Solid-state molecular structures of a) **2**-*Pccn* and b) **3** with 30% thermal probability ellipsoids. Hydrogen atoms are omitted for clarity. Asterisks denote symmetry-generated atoms.

2.442(1) Å) and (η^5:η^5-Pn)$_2$Ti$_2$(CO)$_2$ (Ti-Ti = 2.425(1) Å)[23] that possess titanium-titanium single bonds. However, the Ti-Ti distance in **1**·1.5C_7H_8 is well under the sum of the van der Waals radii ($\Sigma(r_{vdW})$Ti-Ti = 4.3 - 4.92 Å),[33] possibly signifying the presence of a Ti-Ti bond. Consistent with this, the ^{1}H NMR spectrum of **1**·1.5C_7H_8 in C_6D_6 displays a set of diamagnetic resonances.

Treatment of toluene solutions of **1** with 4 equiv. of KC_8 in the presence of small amounts of 1,2-bis(dimethylphosphino)ethane (DMPE) at -35 °C for 5 d yields a mixture of two products in an approximate 2:1 ratio consisting of a paramagnetic and diamagnetic species, respectively. The major product formed from the reaction is paramagnetic **2** (Scheme 1), which can be isolated in 63% yield as dark brown crystals from either concentrated THF/Et_2O or DME/hexanes solutions stored at -35 °C overnight. Persistent attempts to grow crystals of the minor, diamagnetic reaction product failed. The presence of DMPE is necessary for the successful synthesis of **2**, though its role in the reaction is not clear, which is reminiscent of the synthesis of the arene-hafnate [K(18-crown-6)]$_2$[Hf($C_{14}H_{10}$)$_3$] that also requires the presence of a phosphine (PMe_3) for success.[34]

Compound **2** provides polymorphic crystalline material dependent on the solvents of crystallization, yielding crystals in the orthorhombic space group *Pccn* (**2**-*Pccn*) from THF/Et_2O solutions (Figures 2a and S36) and crystals in the triclinic space group $P\bar{1}$ (**2**-$P\bar{1}$) from the combination of DME/hexanes (Figure S37). The former, **2**-*Pccn*, possesses one half molecule in the asymmetric unit, while the latter, **2**-$P\bar{1}$, displays two crystallographically independent half-molecules in its asymmetric unit with both generating the full molecules through inversion symmetry.

Comparison of the two polymorphs reveal the titanium-titanium and titanium-nitrogen distances to be nearly identical. The Ti-Ti distances (avg., 3.07 Å) in **2** are significantly elongated than in **1**·1.5C_7H_8, while exhibiting inequivalent Ti-N_{Im} bridging distances with average lengths of 1.98 and 2.17 Å. Subtle structural changes between the two polymorphs do exist, namely the titanium bonded η^6-aryl ring in **2**-*Pccn* exhibits a boat conformation where the *ipso* and *para* carbon atoms deviate from the ring plane by 11° and 5°, respectively, whereas the masking aryl substituent in **2**-$P\bar{1}$ adopts a puckered ring, similar to that found in **A**[35] and **B**,[21] with an average fold angle of 12.6°, slightly larger than the 10° of **A**. However, the ring fold in **2**-$P\bar{1}$ falls along an *ortho*/*meta* carbon atom vector, unique from the *ipso*/*para* carbon atom fold planes of **A** and **B**. These ring plane distortions are consistent with population of the π*-system. Obvious C_{aryl}-C_{aryl} bonding patterns within the masking Dipp ring, indicative of charge localization, is absent from **2**-*Pccn* with C_{aryl}-C_{aryl} bond lengths ranging from 1.413(4) – 1.439(3) Å (avg., 1.42 Å). The analogous C_{aryl}-C_{aryl} bonds in **2**-$P\bar{1}$ fall over a wider range of 1.390(3) – 1.473(3) Å displaying some 1,4-cyclohexadiene dianion resonance contributions.

Alternatively, addition of 6 equiv of KC_8 to Et_2O solutions of **1** at -35 °C affords a very dark brown solution after 12 h. Analysis of the crude reaction mixture by ^{1}H NMR spectroscopy only shows small amounts of **2** accompanied by a relative increase in the unknown diamagnetic product. Nonetheless, concentrated Et_2O solutions layered with pentanes and stored at -35 °C for 12 h yields small, dark brown plate-shaped crystals of the NMR silent dinuclear titanium complex **3** in 30% isolated yield (Scheme 1).

Complex **3** crystallizes in the monoclinic space group $P2_1/c$ with one half molecule in the asymmetric unit. Its solid-state molecular structure exhibits a [(μ-N-η^6-Im^{Dipp})Ti]$_2$ core analogous to that observed in **2**, with two diethyl ether supported potassium cations coordinating to the opposing face of the titanium-masked Dipp substituents in an η^6-fashion (Figures 2b and S38). The Ti1-Ti1* separation of 3.1578(9) Å and C-C bond lengths (averaged to 1.46 Å) within the masking Dipp ring are appreciably lengthened as compared to **2**.

Inspection of the μ-η^6:η^6-bound Dipp ring in **3** reveals a half-chair conformation with *ipso* atom C2 sitting out of the ring plane with a 23.2° deviation from planarity (Figure 2b). The sum of the angles around atom C2 ($\sum_{C2}$ = 342.3°) indicates pyramidalization at the carbon atom consistent with monoanionic charge localization. The remaining carbon atoms of the coordinated Dipp ring plane show elongated C-C bonds that range from 1.429(3) to 1.463(3) Å that can be rationalized through delocalization of charge through the C3-C10 π-system (Figure 2b).

Based upon bond metrics and our understanding of **A** and **B**, we tentatively assign dimers **2** and **3** as formally containing Ti(III)/Ti(III) and Ti(II)/Ti(II) centers, respectively. In line with this assessment, the ^{1}H NMR spectrum of **2** in C_6D_6 or THF-d_8 displays broad paramagnetically shifted resonances (Figures S6 and S7) over a -40 – 26 ppm window, shifts not unexpected for a Ti(III)/Ti(III) complex with two-unpaired electrons. Preliminary magnetic study of the compounds by SQUID magnetometry show **2** to possess an effective magnetic moment of μ_{eff} = 1.81 μ_B (0.41 cm^3·K·mol^{-1}) at 300 K (Figure S40). This number is significantly lower than the expected value of μ_{eff} = 2.43 μ_B (0.74 cm^3·K·mol^{-1}) for two non-interacting Ti(III) ions (S = 1/2, C = 0.37 cm^3·K·mol^{-1}), strongly suggesting some antiferromagnetic interactions even at room temperature between the two metal centers in **2**. Moreover, the SQUID magnetic analysis of **3** shows an μ_{eff} = 3.26 μ_B (1.34 cm^3·K·mol^{-1}) at 300 K, which is below the 4.0 μ_B (2.0 cm^3·K·mol^{-1}) expected for two isolated Ti(II) ions (S = 1, C = 1.0 cm^3·K·mol^{-1}). Comprehensive electronic study of these systems is currently underway and further detail of their electronic and magnetic properties will be reported in due course.

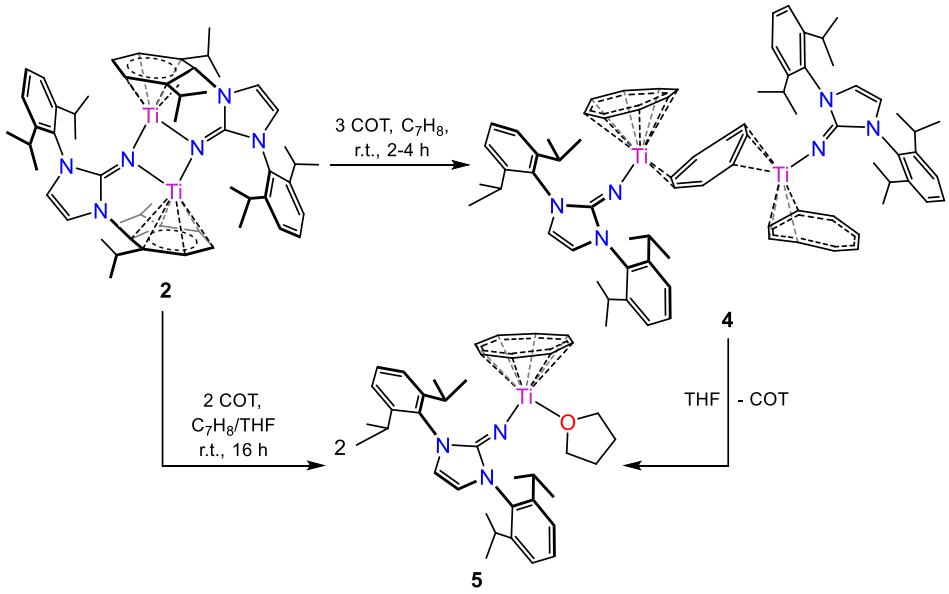

Scheme 2. Reaction of **2** with COT to give **4** and **5**.

Preliminary Reactivity Studies of Reduced Titanium Dimer Complexes 2 and 3. Of note, **2** and **3** can be synthesized under argon or nitrogen atmospheres with no evidence for N_2 binding under standard pressures. These dimers are surprisingly stable in solution, exhibiting no change in C_6D_6 when heated at 80 °C for several weeks. This contrasts the thermal instability of **A**, which undergoes rapid intramolecular C-H activation under these conditions.[35] With respect to **B**, heating its solutions leads to conversion of inter- to intramolecularly masked arene-binding.[21] On this note, we have begun exploring the redox chemistry of **2** and **3** towards π-acids, unsaturated hydrocarbons, namely cyclooctatetraene (COT), and two-electron oxidants such as organoazides.

Exposure of C_6D_6 solutions of **2** to an atmosphere of CO (5 psi) results in the immediate change to an intense red-color with quantitative formation of a new paramagnetic product as observed by ^{1}H NMR spectroscopy (Figure S34). Analogous treatment of **3** with CO in the presence of 2 equiv. of 18-crown-6 affords dark orange-brown solutions with a ^{1}H NMR spectrum that is nearly identical to that observed in the reaction of 2 with CO (Figure S35). Unfortunately, crystallization attempts under a variety of temperatures in multiple solvent mixtures failed for both reactions, yielding either dark powders or oils. Curiously, FTIR measurements do not present obvious CO stretching vibrations. (Figures S55 and S56).

Pressurization of C_6D_6 solutions of **2** under 150 psi H_2 at room temperature does catalyze the formation of $C_6D_6H_6$, presenting chemistry similar to that of **B**.[21] Yet, this results in decomposition of the titanium compound over 12 h. Comparably, exposure of **3** to H_2 under the same reaction conditions does promote the hydrogenation of C_6D_6 to $C_6D_6H_6$, albeit at a much slower rate and also at the expense of the titanium compound.

Reactivity of **2** and **3** with alkynes was explored as cyclotrimerization by low-valent titanium has been extensively documented.[36-42] Treating solutions of either **2** or **3** with excess PhCCPh or $Me_3SiCCSiMe_3$ at variable temperatures resulted in no evident reactivity, while treatment with MeCCMe promotes rapid consumption of the starting materials as reflected by a significant change in coloration from dark brown to dark red. Attempts to characterize the composition of the product were unfruitful with no evidence for the formation of hexamethylbenzene.

In contrast, greater success in producing tractable products was met when using COT with **2** and **3**. Addition of 3 equiv. COT to room temperature toluene suspensions of **2** results in an immediate color change to intense dark red, which evolved into dark brown upon prolonged stirring. Storing concentrated toluene solutions layered with hexanes at -35 °C over 2 d promotes growth of crystalline dark-brown plates corresponding to the inverted sandwich-type species [(Im^{Dipp}N)(η^8-COT)Ti](μ-η^2:η^3-COT)[Ti(η^4-COT)(^{Dipp}NIm)] (**4**) in 73% isolated yield (Scheme 2).

Complex **4**·2C_7H_8 crystallizes in the monoclinic space group $P2_1/n$ with one full molecule accompanied by two disordered toluene equivalents in the asymmetric unit. The molecule is comprised of two [(Im^{Dipp}N)Ti(COT)] fragments bridged by a COT unit (Figure 3). Interestingly, all three COT ligands exhibit distinct hapticities and conformations in the solid-state. While the η^8-COT unit coordinated to Ti1 is slightly puckered, the Ti2 bound η^4-COT and the sandwiched μ-η^2:η^3-COT units display a boat-type conformation. Whereas Zr and Hf complexes displaying η^4-COT and η^4-$C_8H_6(SiMe_3)_2$ units are well-known,[34, 43-48] their titanium counterparts are uncommon.[49-51] Moreover, the η^3-conformation adopted by the sandwiched COT unit in **4** is unique among known titanium-COT complexes.

The simple convention for identifying neutral and dianionic COT conformations, tub-shaped vs. planar,[52] falls short when explaining the dianionic charge assignments in η^4-COT[34, 49, 53] and η^3-COT[34, 49] coordination modes observed in other Group 4 complexes, which is further complicated by the ability of COT to adopt a radical monoanionic state as found in the η^4-COT bound iron complex [PhP($CH_2CH_2PPh_2$)$_2$]Fe(η^4-COT).[54] Unfortunately, poor crystallographic data quality precludes a meaningful

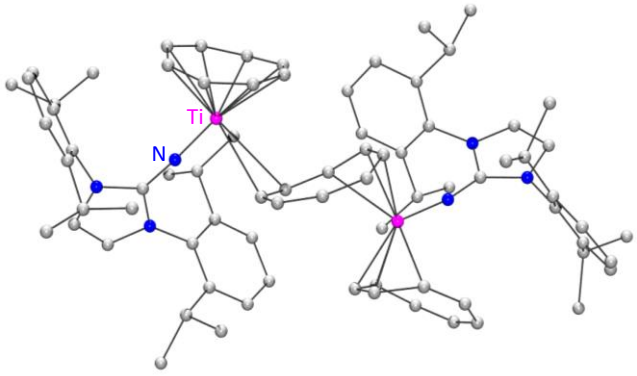

Figure 3. Solid-state molecular structure of **4**·2C_7H_8 presented as ball and stick model to demonstrate connectivity. Hydrogen atoms and co-crystallized toluene molecules omitted for clarity.

analysis of the COT bond metrics; however, preliminary room temperature magnetic measurements by SQUID magnetometry reveal a μ_{eff} = 2.45 μ_B (0.75 $cm^3 \cdot K \cdot mol^{-1}$) (Figure S42) for **4**·2C_7H_8, as would be expected for a Ti(III)/Ti(III) dimer with non-interacting nuclei.

Standing solutions of **4** in THF stored at low temperature for more than 12 h affords thin dark orange plates of the monomeric Ti(III) species ($Im^{Dipp}N$)Ti(η^8-COT)(THF) (**5**) (scheme 2), which crystallizes from THF/hexanes solutions as **5**·0.375C_6H_{14}·0.125THF in the monoclinic space group $P2_1/n$, featuring two independent molecules in the asymmetric unit (Figure 4). Alternatively, **5**·0.375C_6H_{14}·0.125THF can be accessed directly in 76% yield from the reaction of **2** with 2 equiv. COT in toluene at room temperature for 12 h followed by recrystallization in THF/hexanes (Scheme 2).

Comparison of **5**·0.375C_6H_{14}·0.125THF with the Ti(IV) complex ($Im^{Dipp}N$)Ti(η^8-COT)Cl and the isostructural Sc species ($Im^{Dipp}N$)Sc(η^8-COT)(THF) reveals similar COT ring puckering and average C-C bond lengths of 1.400(5) Å, 1.40(2) Å, and 1.40(2) Å,[55] respectively, denoting the localization of dianionic charge in the COT unit and 3+ oxidation state of the titanium center in **5**·0.375C_6H_{14}·0.125THF. This is in agreement with the paramagnetic behavior observed in its ^{1}H NMR spectrum (Figure S10).

Inspection of the M-C_{cent}, M-N_{Im} distances, and M-N_{Im}-C angle reveal significantly shorter metal-ligand separations and a slightly narrower bending angle in **5**·0.375C_6H_{14}·0.125THF (Ti1-C_{cent} = 1.527(3) Å; Ti1-N1 = 1.941(2) Å, Ti1-N1-C9 = 162.0(2)°) as compared to ($Im^{Dipp}N$)Sc(η^8-COT)(THF) (Sc-C_{cent} = 1.617(3) Å; Sc-N_{Im} = 1.97(1) Å; Sc-N_{Im}-C_{Im} = 167(1)°), suggesting a stronger bonding interaction of titanium with the COT^{2-} and $Im^{Dipp}N^-$ ligands. In comparison to the more oxidized Ti(IV) species ($Im^{Dipp}N$)Ti(η^8-COT)Cl, it displays a significantly shorter Ti-N_{Im} bond length (1.79(2) Å) and more acute M-N_{Im}-C angle (149.5(1)°).

Of note, the room temperature ^{1}H NMR spectra of both **4**·2C_7H_8 and **5**·0.375C_6H_{14}·0.125THF are nearly identical (Figures S8 and S10), indicating that the dimeric structure of **4** is not preserved in solution. We posit that the loss of the bridging COT ligand is facile in solution, leading to the formation of coordinatively unsaturated ($Im^{Dipp}N$)(η^8-COT)Ti, not dissimilar to the structurally characterized zirconium pogo-stick complex (η^7-C_7H_7)($Im^{Dipp}N$)Zr.[56] This would explain the formation of **5** from **4** in standing THF solutions, where the coordinating solvent readily displaces the neutral COT. Variable temperature ^{1}H NMR

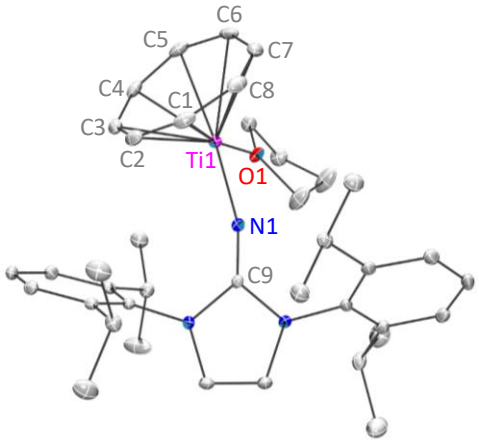

Figure 4. Solid-state molecular structure of one molecule of **5**·0.375C_6H_{14}·0.125THF with 30% probability ellipsoids. Hydrogen atoms and co-crystallized solvent molecules are omitted for clarity. Selected bond lengths (Å) and angles (deg): Ti1-N1 = 1.941(2), Ti1-C_{cent} = 1.525(3), N1-C9 = 1.254(3), Ti1-N1-C9 = 162.0(2).

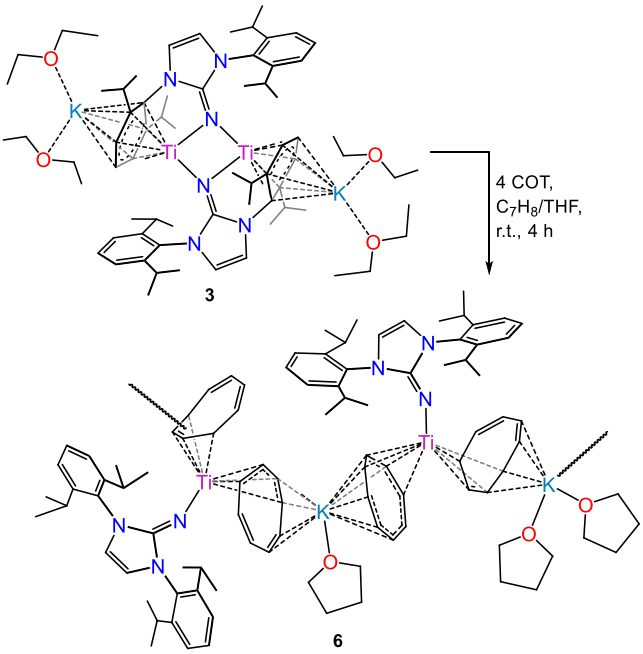

Scheme 3. Synthesis of **6** from **3.**

spectroscopy in tol-d_8 of **4**·2C_7H_8 shows signal sharpening and decoalescence of resonances upon cooling to -50 °C, allowing for the identification of two separate sets of resonances attributable to two distinct COT environments (Figure S9).

Room temperature reactions of **3** with 4 equiv. COT in toluene/THF solution yield crystals of a one dimensional polymeric species formed by repeating [($Im^{Dipp}N$)(η^4-COT)Ti(μ-η^4:η^6-COT)K(THF)(μ-η^5:η^4-COT)Ti(NIm^{Dipp})(μ-η^4:η^4-COT)K$(THF)_2$]$_n$ (**6**) units as shown through X-ray crystallographic analysis (Scheme 3). Complex **6**·0.7THF·0.15C_6H_{14} crystallizes in the triclinic $P\bar{1}$ space group with one complete molecule in the asymmetric unit containing two titanium centers, each connected to two COT and one imidazolin-2-iminato ligands, brought together by interaction of bridging potassium cations with the COT rings (Figure 5). All four COT units in **6**·0.7THF·0.15C_6H_{14} exhibit an intermediate conformation between half-chair and boat with variable degrees of deviation from planarity (Figure 5). Inspection of the C-C bonds within the COT rings show two of the moieties to possess localized -ene dianion character through η^4-coordination to the titanium centers while the remaining COT ligands exhibit charge delocalization that coincides with the greater planarity of those rings.

Regardless of the differing coordination environments in the solid-state, the ^{1}H NMR spectrum of **6**·0.7THF·0.15C_6H_{14} in C_6D_6 shows a diamagnetic compound with the resonance corresponding to the COT protons appearing as a single peak at 5.39 ppm, indicating equivalence in solution (Figure S11). Consistent with this notion, a signal assignable to the carbon atoms of the COT ring does not appear in the $^{13}C\{^1H\}$ NMR spectrum due to high fluxionality on the NMR timescale. Similar proton equivalence has been observed in NMR studies performed on the mixed-hapticity zirconium and hafnium COT species Zr(η^8-COT)(η^4-COT) (5.95 ppm, CD_2Cl_2)[47] and [$K(THF)_{0.5}$]$_2$[Hf(η^3-COT)$_2$(η^4-COT)] (5.00 ppm, THF-d_8).[34]

Together, the formation of **4**, **5**, and **6** unequivocally demonstrates the ability of **2** and **3** to behave as low-valent titanium synthons capable of transferring reducing equivalents to multiple COT ligands. In the case of **4** and **5** containing trivalent titanium centers, the reactions occur through four-electron oxidation of **2**, positioning it as a monovalent "Ti(I)/Ti(I)" synthon. With respect to **6**, it arises from the two-electron reduction of 4 COT ligands, providing in sum an 8-electron oxidation of **3** that produces a

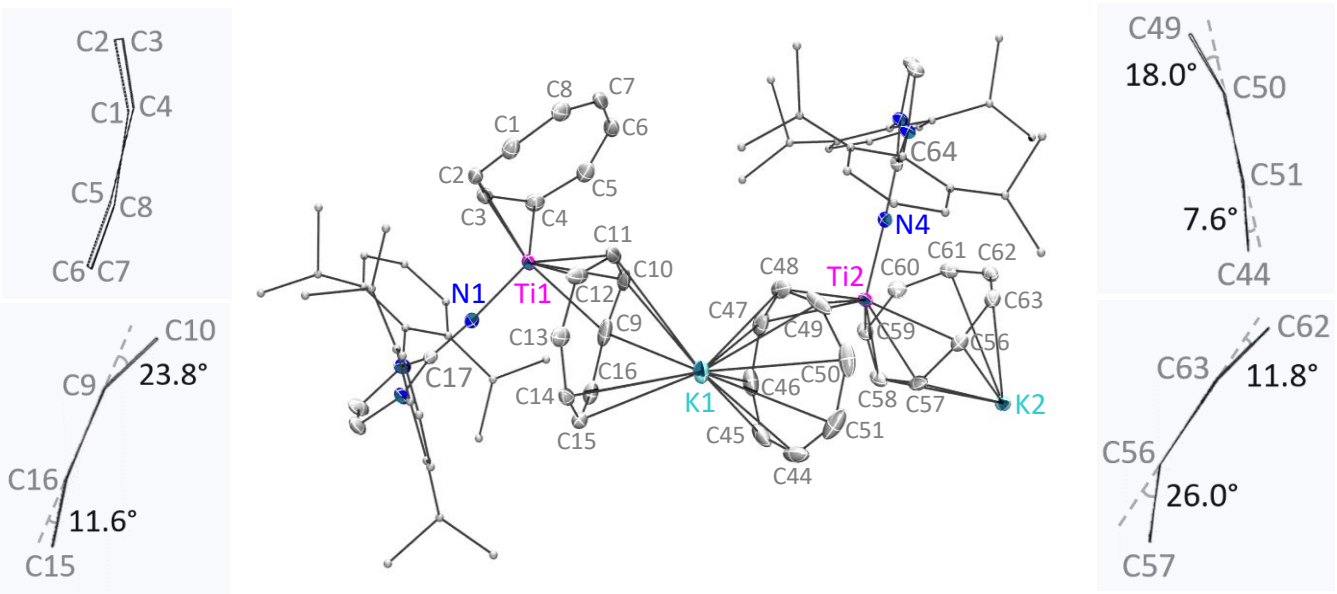

Figure 5. Solid-state molecular structure of one molecule of **6**·0.7THF·0.15C_6H_{14} with 30% probability ellipsoids. Hydrogen atoms and co-crystallized solvent molecules are omitted for clarity. Selected bond lengths (Å) and angles (deg): Ti1-N1 = 1.845(2), Ti1-C1 = 2.433(3), Ti1-C2 = 2.222(3), Ti1-C3 = 2.266(3), Ti1-C4 = 2.688(3), Ti1-C9 = 2.413(3), Ti1-C10 = 2.268(3), Ti1-C11 = 2.297(3), Ti1-C12 = 2.524(4), Ti2-N4 = 1.845(2), Ti2-C47 = 2.569(4), Ti2-C48 = 2.225(3), Ti2-C49 = 2.237(3), Ti2-C50 = 2.686(4), Ti2-C56 = 2.451(3), Ti2-C57 = 2.285(3), Ti2-C58 = 2.281(3), Ti2-C59 = 2.400(3), Ti1-N1-C17 = 172.6(2), Ti2-N4-C64 = 171.8(2).

dimer possessing tetravalent titanium, therefore establishing **3** as a zerovalent "Ti(0)/Ti(0)" synthon.

Discrete Ti(I) compounds are exceedingly rare and limited to the arene sandwich complexes [(η^6-1,3,5-^{i}Pr$_3$C$_6$H$_3$)$_2$Ti][BAr] (BAr = C_6H_5, p-C_6H_4F, 3,5-$C_6H_3(CF_3)_2$).[42, 57] Therefore, our system offers a novel entry point for examining the reactivity of monovalent titanium. On the other hand, Ti(0) complexes, stabilized by π-acceptors such as CO or arenes, are well established though relatively few in number,[58-59] paling in comparison to the known chemistry of Ti(II), Ti(III), and Ti(IV) compounds.

Further probing the chemistry of these highly reduced dimers, the reaction of **2** and **3** with organoazides was explored. For instance, addition of 3 equiv of 1-azidoadamantane (AdN_3) to a toluene suspension of **2** at -35 °C results in immediate gas evolution accompanied by formation of a dark-red, soluble product. Concentration of the solution and layering with hexanes stored at -35 °C for several days produces crystalline red blocks of the dinuclear tris(imido) species [(Im^{Dipp}N)Ti(=NAd)](μ-NAd)$_2$[Ti(^{Dipp}NIm)(N_3Ad)] (**7**) (Scheme 4). Compound **7** forms from the 6-electron reduction of three molecules of AdN_3, giving a compound featuring one terminal and two bridging imido ligands with a site on the non-terminal imido coordinated titanium occupied by a neutral molecule of AdN_3. Surprisingly, repeating the reaction with 4 equiv of AdN_3 leads to an insignificant improvement in the total yield. Compound **7** is exceedingly soluble in aromatic, ethereal, and non-polar solvents such as pentane and hexanes. As a result of this, lengthy crystallizations are required to isolate it in reasonable amounts.

Complex **7**·3C_7H_8 (Figure 6a) crystallizes in the monoclinic space group $P2_1/c$ with an asymmetric unit composed of three co-crystallized toluenes and a full molecule of **7** that depicts disorder of the coordinated AdN_3 unit over two positions. The poor quality of the refinement parameters, namely a high weighted R-factor (wR2 = 27.30%), prevents consequential analysis of its metrical parameters. Nonetheless, the bond metrics point to a clear asymmetry in the bridging titanium-imido bond lengths, where the Ti1-N_{bridge} bonds are approximately 0.25 Å longer than the Ti2-N_{bridge} distances, pointing to significant multiple bond character in the latter.

The ^{1}H NMR spectra of product mixtures of **7**·3C_7H_8 are always accompanied by the presence of another minor, diamagnetic product that exhibits sharp resonances consistent with a low-symmetry, adamantyl-containing species with a distinctive set of aromatic resonances. This product can be selectively synthesized by carrying out the reaction of **2** with 3 equiv of AdN_3 in toluene at room temperature for 12 h, giving red/yellow solutions of the aryl C-H activated product [(Im^{Dipp}N)Ti(NHAd)](μ-NAd)$_2$[Ti(C_6H_4Me)(^{Dipp}NIm)] (**8-tol**) in 73% yield (Scheme 4).

X-ray diffraction analysis shows **8-tol** to crystallize in the orthorhombic space group $P2_12_12_1$ accompanied by highly disordered solvent molecules of crystallization (Figure 6b). The asymmetric unit possesses one full molecule of **8-tol** with crystallographic disorder at the tolyl ligand, showing regioselective C-H activation at the *meta* and *para* positions in a 7:3 ratio, respectively. Complex **8-tol** exhibits a Ti$_2$(μ-NAd)$_2$ diamond core with each metal center additionally coordinating one terminal Im^{Dipp}N ligand. The Ti1-N3 = 1.912(2) Å bond distance and Ti1-N3-C21 = 143.8(2)° angle reveal an adamantyl-amido group. This Ti-NHAd bond in **8-tol** is slightly elongated compared to the only other crystallographically characterized titanium adamantyl-amido complex *trans*-C_6H_4-{1,2-[*N*,2-*N*(Dipp)-C_6H_4]$_2$Ti-NHAd}$_2$ (Ti-N_{HAd} = 1.886(3) Å, Ti-N_{HAd}-C_{Ad} = 140.63(19)°).[60] The Ti2-C31 = 2.157(3) Å bond distance is unremarkable and falls within the range of structurally characterized titanium-tolyl bonds found in [*p*-^{t}Bu-calix[4]-(OMe)$_2$-(O)$_2$Ti(*p*-MeC_6H_4)] (2.110(7) Å),[61] [(*o*-MeC_6H_4)Ti(O^{i}Pr)$_2$(μ-O^{i}Pr)]$_2$ (2.134(4) Å),[62] and [(C_5H_5)$_2$Ti(*p*-MeC_6H_4)]$_2$$N_2$ (2.216(7) Å).[63] Structural analysis within the core shows slightly shorter metal-imido bonds for the tolyl-coordinated titanium atom (Ti2-N1 = 1.906(4) Å, Ti2-N2 = 1.905(4) Å) than for the amido-coordinated metal atom (Ti1-N1 = 1.949(4) Å, Ti1-N2 = 1.962(4) Å).

Resonances assignable to the amido proton appear closely at 6.64 and 6.65 ppm for the two regioisomers of **8-tol** in its room temperature ^{1}H NMR spectrum in C_6D_6 (Figure S19). Moreover, the signals corresponding to the methyl protons of the tolyl moiety appear for the *meta*- and *para*-isomers at 2.47 and 2.26 ppm, respectively.

Toluene metallation to form regioisomeric mixtures is precedented.[64-65] For example, [(tmeda)Na(μ-^{t}Bu)(μ-tmp)Zn(^{t}Bu)][64] (tmp = 2,2,6,6-tetramethylpiperidine) reacts with toluene to yield

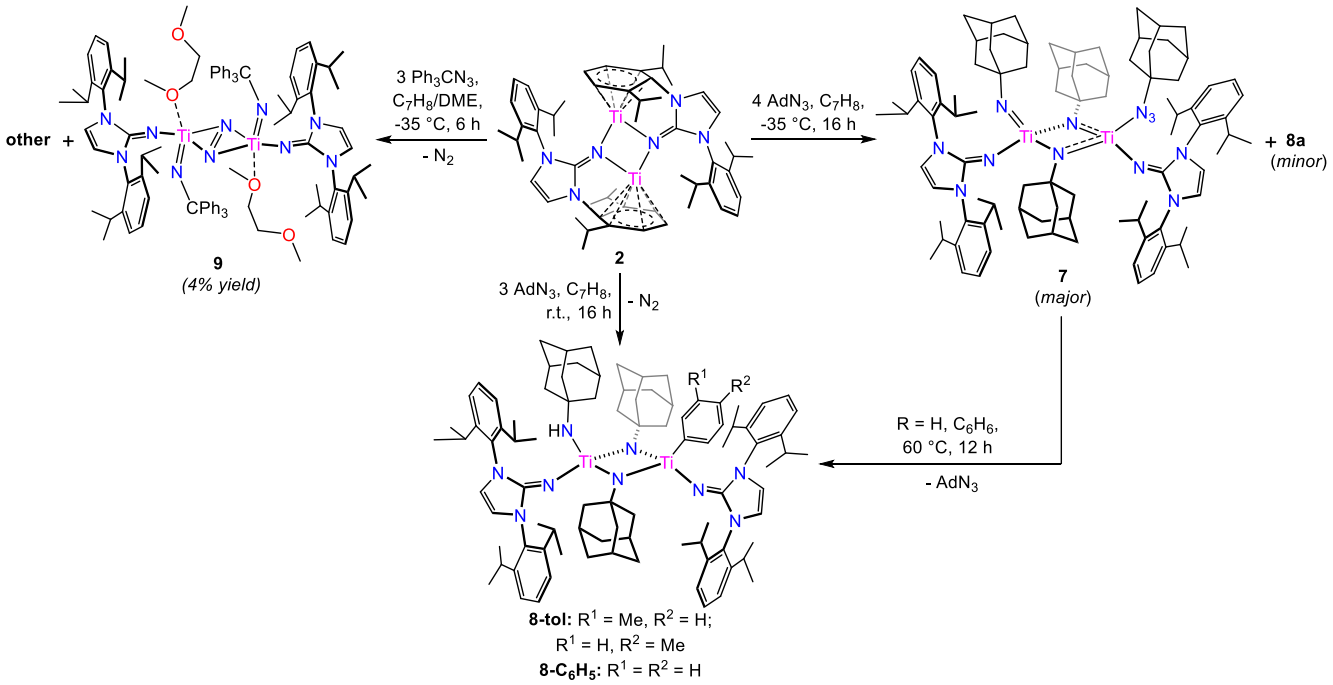

Scheme 4. Reactivity of **2** with organoazides to yield **7** – **9**.

a regioselective mixture of the *meta*- and *para*- toluene insertion products [(tmeda)Na(μ-$C_6H_4CH_3$)(μ-tmp)Zn(^{t}Bu)] in a 64.5:35.5 ratio accompanied by isobutane formation.[64] Similarly, selective *meta*- over *ortho*- C-H activation of toluene by the β-diketiminate aluminum complex (^{Dipp}BDI)Al (^{Dipp}BDI = CH[C(CH_3)N(Dipp)]$_2$) takes place at room temperature in the presence of catalytic amounts of the calcium hydride compound [(^{Dipp}BDI)Ca(H)]$_2$.[65]

The intermolecular C-H activation of aromatic and aliphatic hydrocarbons by group 4, d^0 terminal metal-imido complexes is well documented.[30, 66-73] Based upon this, **7** and **8-tol** may be delineated as the respective kinetic and thermodynamic products of the reaction of **2** with AdN_3 in toluene, where terminal imido **7** is an intermediate in the formation of **8-tol**. To test this, C_6D_6 solutions of **7** were heated to 60 °C. After 12 h, complete consumption of the starting material and formation of the expected benzene C-D activated product [(Im^{Dipp}N)Ti(NDAd)](κ^2-NAd)$_2$[Ti(C_6D_5)(^{Dipp}NIm)] (**8-C_6D_5**) was observed (Scheme 4, Figure S28). Moreover, conversion of **7** to **8-tol** was observed to happen even at -35 °C over the course of several days (Figure S29) or at room temperature after 60 h.

Complex **8-C_6H_5** can be prepared in 60% yield independently using a synthetic procedure analogous to that used to make **8-tol** and exhibits comparable solubility and structural features (Figure S39). Its phenyl protons appear as a doublet at 8.20 ppm (*ortho* H) with overlapping signals at 7.27-7.33 ppm (assignable to the 3 *meta* and *para* hydrogens); while the N-H proton of its adamantyl-amido is observed as a singlet at 6.65 ppm (Figure S23).

The successful 6-electron oxidation of **2** to produce **7** and **8** encouraged us to explore the reactivity of **2** towards a more sterically encumbering and more electron deficient azide. In this regard, the 6 h reaction of **2** with 3 equiv of Ph_3CN_3 in toluene at -35 °C yields dark red-yellow solutions. The ^{1}H NMR spectral characterization of the crude material revealed the presence of a complicated mixture of products. A small amount of orange crystals in trace yield (4%) of the dinitrogen bridged titanium trityl imido complex [(Im^{Dipp}N)Ti(NCPh$_3$)(κ^1-DME)]$_2$(μ-η^2:η^2-N_2) (**9**) were obtained after evaporation and crystallization from DME at -35 °C (Scheme 4).

Complex **9** crystallizes in the monoclinic space group $P2_1/c$ with one half molecule contained in the asymmetric unit (Figure 7). The full molecule, generated by crystallographic mirror symmetry, consists of two [(Im^{Dipp}N)Ti(NCPh$_3$)(DME)]$^{n+}$ fragments bridged by a side-on bound N_2 unit. The titanium-imido distance Ti1-N5 = 1.736(1) Å is longer than that found for the only other crystallographically characterized titanium trityl imido complex (salophen)Ti(NCPh$_3$) (salophen = [1,4-(1-O-C_6H_4-2-CHN)$_2$-C_6H_4]$^{2-}$) with its shorter Ti-N = 1.686(4) Å bond length. The titanium-imidazolin-2-iminato distance of Ti1-N2 = 1.900(1) Å is elongated in comparison to the Ti-N_{Im} = 1.845(2) Å bonds in **6**. These longer titanium-nitrogen bonds in **9** may be due to steric congestion at the metal center, which further manifests in monodentate coordination of the DME ligand. Its solid-state structure reveals a planar Ti1-(μ-η^2:η^2-N_2)-Ti1* core with slightly different Ti-N bond lengths (Ti1-N1 = 2.089(1), Ti1-N1* = 2.135(1) Å) with a N1-N1* separation of 1.236(3) Å.

Insights regarding the extent of N_2 reduction cannot be provided on the sole basis of bond metric analysis as demonstrated by the rather contrasting electronic assignments reported for other group 4 bimetallic complexes featuring side-on bound N_2 units. For instance, while side-on N_2 coordinated titanocene complexes [(η^5-C_5H_2-1,2,4,-Me$_3$)$_2$Ti]$_2$(μ,η^2,η^2-N_2) (N-N = 1.216(4) Å),[74] and [(η^5-C_5H_3-1-^{i}Pr-3-R)$_2$Ti]$_2$(μ,η^2,η^2-N_2) (R = Me, N-N = 1.217(6) Å; R = ^{i}Pr, N-N = 1.226(6) Å)[75] were found to be paramagnetic at room temperature with moderately activated $(N_2)^{2-}$ bridging units; the titanium dimer [{[(Me$_3$Si)$_2$N]$_2$Ti}$_2$(μ-η^2:η^2-N_2)$_2$][Li(TMEDA)$_2$] displays a much more elongated N-N bond of 1.38(2) Å in length,[76] which was suggested to be neutral despite this complex exhibiting a low effective magnetic moment of 1.37 μ_B and formally having 5 metal-based electrons available for donation to the N_2. This is significantly differentiated from the dimeric zirconium and hafnium dinitrogen species {(η^5-C_5Me_4H)Hf[N(^{i}Pr)C(Me)N(^{i}Pr)](Br)}$_2$(μ-η^2:η^2-N_2) (N-N = 1.253(3) Å),[77] [(η^5-C_5Me_4H)$_2$Zr]$_2$(μ-η^2:η^2-N_2) (N-N = 1.377(3) Å),[78] and {[η^5-C_5H_3-1,3-(SiMe$_3$)$_2$]$_2$Zr}$_2$(μ-η^2:η^2-N_2) (N-N = 1.47(3) Å),[79] all of which are described as possessing $(N_2)^{2-}$ moieties.

Similar discrepancies have also been observed in Ln and 3*d*-metal based bridging N_2 dimers with N-N bond lengths comparable to that observed in **9**. For example, while the M-(μ-η^2:η^2-N_2)-M interaction observed in {[CyNC(H)NCy]$_2$V}$_2$(μ-η^2:η^2-N_2) (N-N = 1.235(6) Å) was found to be labile in THF solutions,[80] resulting in N_2 loss and formation of monomeric species [CyNC(H)NCy]$_2$V(THF)$_2$; the N_2 units in octaethylporphyrinogen

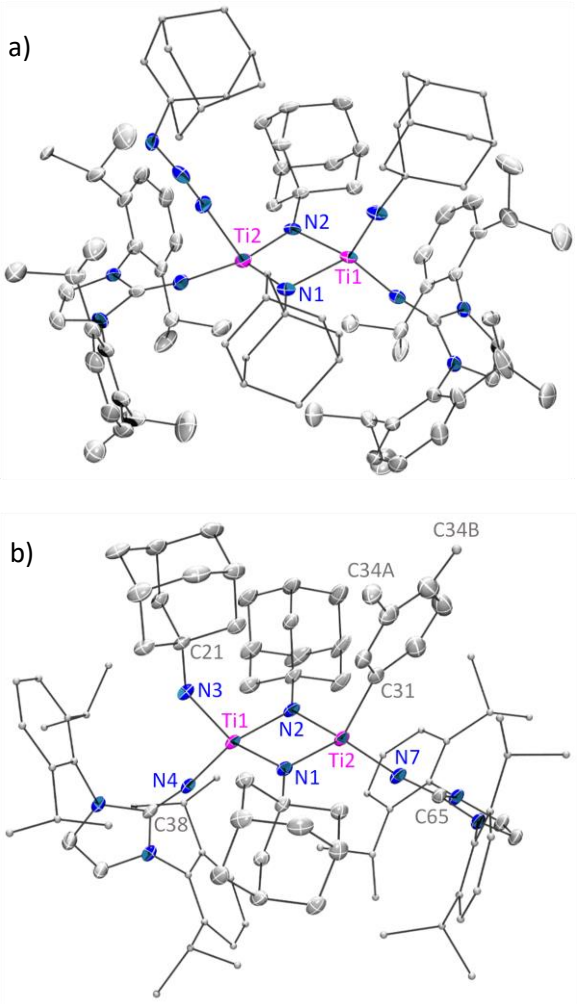

Figure 6. Solid-state molecular structure of a) **7**·3C_7H_8 presented for connectivity and b) **8-tol** with 30% probability ellipsoids. Hydrogen atoms and co-crystallized solvent molecules are omitted for clarity. Selected bond lengths (Å) and angles (deg) for **8-tol**: Ti1-Ti2 = 2.8450(7), Ti1-N1 = 1.948(2), Ti1-N2 = 1.959(2), Ti1-N3 = 1.912(2), Ti1-N4 = 1.878(2), Ti2-N1 = 1.909(2), Ti2-N2 = 1.908(2), Ti2-N7 = 1.875(2), Ti2-C31 = 2.157(3), Ti1-N3-C21 = 143.8(2), Ti1-N4-C38 = 164.7(2), Ti2-N7-C65 = 172.8(2).

(Et_8N_4) supported lanthanide complexes [{[(η^5:η^1:η^1:η^5-Et_8N_4)Nd][Na(diox)][Na(diox)$_2$]}$_2$(μ-η^2:η^2-N_2) (N-N = 1.234(8) Å), and [{[(η^5:η^1:η^1:η^5-Et_8N_4)Pr][Na(DME)]}$_2$(μ-η^2:η^2-N_2)][Na(DME)$_3$]$_2$ (N-N = 1.254(7) Å) were found to be reduced by two electrons with the dimeric structures being preserved under vacuum.[81]

Complex **9** is unusual as we are not aware of any other metal compounds possessing side-on bound N_2 that also feature metal-ligand multiple bonds. The formation of **9** is not understood and is obfuscated by its trace yield and the complex mixture of products generated in the reaction of **2** with Ph_3CN_3. The origin of the bridging N_2 ligand likely arises from the reduction of the N_2 atmosphere used in the reaction; however, it cannot be discounted that the N_2 is captured from the dinitrogen released from reduction of an azide unit. Gomberg's dimer is not detected in the crude product mixture, thus making the formation of intermediate nitride species unlikely.

Reacting toluene suspensions of **3** with 4 equiv of AdN_3 affords dark red solutions, which upon addition of 2 equiv of 18-crown-6 and dissolution into THF/pentane followed by storage at -35 °C for several days yields crystalline pink-orange blocks. Single crystal X-ray diffraction analysis revealed the formation of the dinuclear tris(imido) complex [K(18-crown-6)(THF)$_2$]{[(Im^{Dipp}N)Ti(NAd)](μ-NAd)$_2$K[Ti(NIm^{Dipp})]} (**10**) (Scheme 5), which is shown in Figure 8. The compound, **10**·THF, crystallizes in the triclinic space group $P\bar{1}$ with molecules of THF in the asymmetric unit. The solid-state molecular structure is comprised of a charge separated [K(18-crown-6)(THF)$_2$]$^+$ and [(Im^{Dipp}N)Ti(NAd)](μ^2-NAd)$_2$K[Ti(NIm^{Dipp})]$^-$ cation/anion pair, where the anionic fragment consists of a heterotrimetallic cluster with two titanium centers that incorporates a second potassium cation. The core features of the anionic fragment of **10**·THF are qualitatively similar to those found for **7**·3C_7H_8. Specifically, the anion consists of a Ti_2(μ-NAd)$_2$ diamond core with one of the titanium atoms possessing a terminal adamantyl imido ligand with a Ti1-N3 = 1.729(3) Å bond distance that is comparable to the corresponding Ti1-N3 ≈ 1.73 Å bond in **7**·3C_7H_8. Additionally, the notable asymmetry observed in the Ti_2(μ-NAd)$_2$ diamond core of **7**·3C_7H_8 appears in **10**·THF, where the Ti1-N1 = 2.064(3) Å and Ti1-N2 = 2.029(3) Å pair of bonds is significantly longer than the Ti2-N1 = 1.845(3) Å and Ti2-N2 = 1.865(3) Å bond set. In place of the coordinated AdN_3 of **7**·3C_7H_8, the potassium cation sits within the immediate coordination sphere of the titanium, featuring a short titanium-potassium contact distance of Ti1-K1 = 2.349(1) Å that is held in place through interactions with the neighboring ligated nitrogen atoms.

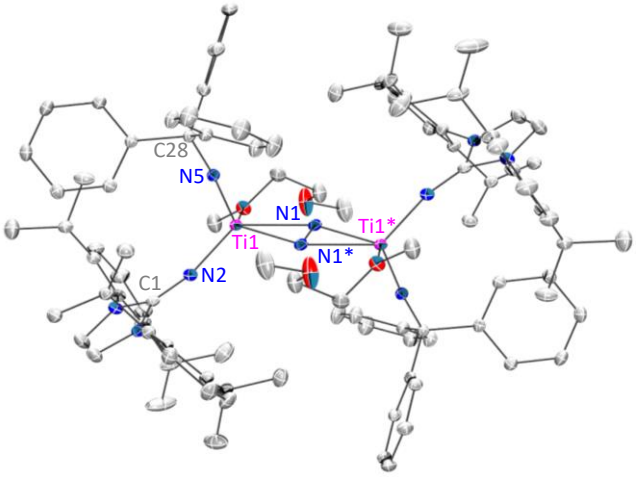

Figure 7. Solid-state molecular structure of **9** with 30% thermal probability ellipsoids. Hydrogen atoms and co-crystallized solvent molecules are omitted for clarity. Asterisks denote symmetry generated atoms. Selected bond lengths (Å) and angle (deg): Ti1-N1 = 2.089(1), Ti1-N1* = 2.135(1), N1-N1* = 1.236(3), Ti1-N5 = 1.736(1), N5-C28 = 1.448(2). Ti1-N2 = 1.900(1), N2-C1 = 1.275(2), Ti1-N5-C28 = 173.5(1), Ti1-N2-C1 = 173.5(1).

Compound **10** forms through the 6-electron reduction of three molecules of AdN_3, thus giving a Ti(III)/Ti(III) complex. However, the ^{1}H NMR spectrum of **10**·THF in C_6D_6 shows a series of broadened resonances that fall within the diamagnetic window in the expected chemical shift regions. Evans method gives an μ_{eff} = 0 μ_B, further confirming the diamagnetic character of **10**. The Ti1-Ti2 = 2.8446(8) Å interatomic distance is 0.23 Å greater than that of diamagnetic **1**·1.5C_7H_8 with its Ti(III)/Ti(III) centers, but the titanium-titanium distance of **10**·THF is well within the sum of the van der Waals radii (vide supra) and shorter than that found in diamagnetic [CyNC(H)NCy]$_4Ti_2Cl_2$ (Cy = C_6H_{11}) that is described as possessing a Ti-Ti single bond (Ti-Ti = 2.942(2) Å).[82-83] Therefore, the diamagnetic character of **10** can be reasonably explained through the presence of a titanium-titanium bond where the peak broadening in its NMR spectra is likely due to fluxional behavior in solution.

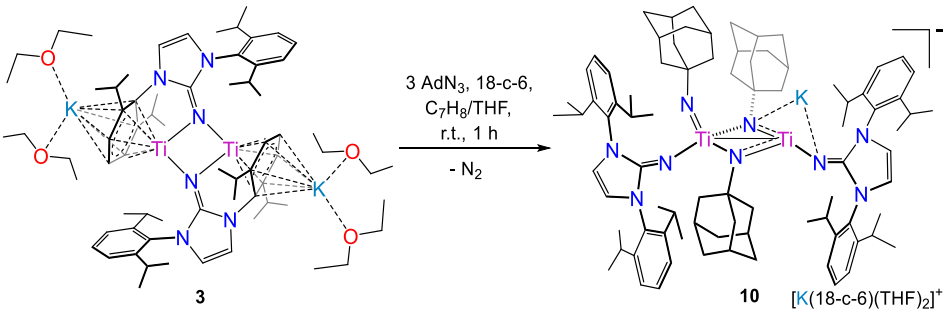

Scheme 5. Reaction of **3** with AdN_3 to form Ti(III)/Ti(III) imido **10**.

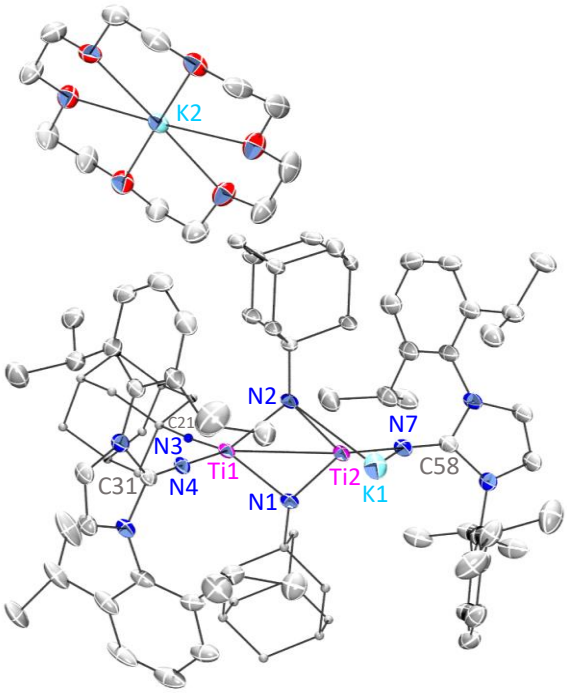

Figure 8. Solid-state molecular structure of **10**·THF with 30% thermal probability ellipsoids. Hydrogen atoms and coordinated and co-crystallized THF molecules are omitted for clarity. Selected bond lengths (Å) and angle (deg): Ti1-Ti2 = 2.8446(8), Ti1-N1 = 2.064(3), Ti1-N2 = 2.029(3), Ti1-N4 = 1.943(3), Ti1-N3 = 1.729(3), Ti2-K1 = 2.349(1), Ti2-N1 = 1.845(3), Ti2-N2 = 1.865(3), Ti2-N7 = 1.907(3), Ti1-N3-C21 = 176.5(3), Ti1-N4-C31 = 173.0(2), Ti2-N7-C21 = 168.6(3).

SUMMARY

The accumulation of charge within multimetallic assemblies or in metal-metal multiple bonds is an effective strategy for accomplishing transfers of 4 or more electrons, which is very important in the context of the activation of small molecules such as O_2, N_2, and CO_2 that require multiple reducing equivalents for bond cleavage. Our group has demonstrated that the two-electron reduced titanium complexes (^{Arket}guan)Ti(η^6-NIm^{Dipp}) (^{Arket}guan = [(^{t}Bu$_2$CN)C(NAr)$_2$]$^-$, Ar = C_6H_3-2,6-^{i}Pr$_2$ (**A**), C_6H_3-3,5-Me$_2$ (**B**); Im^{Dipp}N = [1,3-bis(Dipp)imidazolin-2-iminato]$^-$, Dipp = NC_6H_3-2,6-^{i}Pr$_2$) are potent reductants where the electron-transfer chemistry is enabled by the redox non-innocence of the imidazolin-2-iminato ligand.[20-22, 35] In its hexahapto (η^6-Im^{Dipp}N) ligation mode, the ligand formally possesses trianionic charge with two-electrons stored in a dearomatized, masking Dipp ring. We posited that simplifying our titanium starting materials to exclude the ketimine-guanidinate ligand followed by reduction would yield access to reduced titanium clusters capable of transferring more than two-electrons.

Reduction of (Im^{Dipp}N)TiCl$_3$ with sodium amalgam produces the dinuclear titanium complex [Cl$_2$Ti(μ-NIm^{Dipp})]$_2$ (**1**) that can be further reduced by 4 or 6 equiv. of KC_8 to give [(μ-N-μ-η^6-Im^{Dipp})Ti]$_2$ (**2**) and {[(Et$_2$O)$_2$K](μ-N-μ-η^6:η^6-Im^{Dipp})Ti}$_2$ (**3**), respectively, in modest yields. Compounds **2** and **3** are reactive towards equivalents of cyclooctatetraene (COT), producing [(Im^{Dipp}N)(η^8-COT)Ti](μ-η^2:η^3-COT)[Ti(η^4-COT)(^{Dipp}NIm)] (**4**), (Im^{Dipp}N)Ti(η^8-COT)(THF) (**5**), and [(Im^{Dipp}N)(η^4-COT)Ti(μ-η^4:η^6-COT)K(THF)(μ-η^5:η^4-COT)Ti(NIm-^{Dipp})(μ-η^4:η^4-COT)K(THF)$_2$]$_n$ (**6**). These compounds are formed from 4, 6, and 8-electron transfer processes, establishing **2** and **3** as Ti(I)/Ti(I) and Ti(0)/Ti(0) synthons, respectively. Additional reactivity is observed between **2** with AdN_3 or Ph_3CN_3, generating the Ti(IV)/Ti(IV) imido species [(Im^{Dipp}N)Ti(=NAd)](μ-NAd)$_2$[Ti(^{Dipp}NIm)(N$_3$Ad)] (**7**), [(Im^{Dipp}N)Ti(NHAd)](μ-NAd)$_2$[Ti(C$_6$H$_4$Me)(^{Dipp}NIm)] (**8-tol**), and [(Im^{Dipp}N)Ti(NCPh$_3$)(κ^1-DME)]$_2$(μ-η^2:η^2-N$_2$) (**9**) via 6-electron transfer mechanisms. Of note, **7** is found to be the kinetic product of the reaction of **2** with AdN_3, that upon prolonged standing or heating in toluene solutions, generates the thermodynamically favored **8-tol**. Finally, **3** reacts with 3 equiv of AdN_3 to give the diamagnetic Ti(III)/Ti(III) tris(imido) [K(18-crown-6)(THF)$_2$][[(Im^{Dipp}N)Ti(NAd)](μ-NAd)$_2$K[Ti(NIm^{Dipp})]] (**10**), formed from 6-electron oxidation of **3**.

These results clearly indicate that early-metal compounds can be reduced to form isolable multi-metallic species capable of effecting multi-electron transfer chemistry, including an impressive 8-electron transfer capacity in the case of **3**. Efforts to elucidate the electronic structures of **2** and **3** are underway along with additional reactivity studies.

EXPERIMENTAL SECTION

General Considerations. All air- and moisture-sensitive operations were carried out in a MBraun glovebox under an atmosphere of ultra-high purity nitrogen. Toluene, hexanes, *n*-pentane, tetrahydrofuran (THF), diethyl ether (Et$_2$O), and dimethoxy ethane (DME) solvents were dried using a Pure Process Technology Solvent Purification System and subsequently stored under a dinitrogen atmosphere over activated 4 Å molecular sieves for at least 24 h prior to use. The deuterated solvents, C_6D_6, THF-d_8, and toluene-d_8 were purchased from Cambridge Isotope Laboratories Inc., degassed via three freeze-pump-thaw cycles, and dried over activated 4 Å molecular sieves for over 24 h prior to use. Celite and 4 Å molecular sieves were heated under dynamic vacuum to 150 ºC for over 72 h and then cooled under vacuum. Ultra-high purity H_2 (Alphagaz Grade 1) and Ultra-high purity (99.9%) CO were purchased from Air Liquide America L.P. Houston, TX and used without further purification. (Im^{Dipp}N)TiCl$_3$[84] and Ph_3CN_3[85] were synthesized following reported procedures. Cyclooctatetraene (COT) was degassed via three freeze-pump-thaw cycles and dried over activated 4 Å molecular sieves for over 24 h prior to use. 18-crown-6 was purchased from Oakwood Products, Inc. and made anhydrous using the Gokel method.[86] All other reagents were purchased from commercial sources and used as received. NMR spectra were recorded on a Bruker AVANCE III 400 MHz spectrometer. ^{1}H and ^{13}C{^{1}H} NMR spectra are referenced to $SiMe_4$ using the residual ^{1}H solvent peaks as internal standards or the characteristic ^{13}C signals of the solvent. In addition, resonance assignments in the ^{13}C{^{1}H} NMR spectra are based upon ^{1}H-^{13}C HSQC 2D correlation

spectra. IR data were collected with powdered KBr, pressed into a pellet, or as a neat film sandwiched between NaCl plates, and the data was collected within a few minutes of sample preparation. The intensities are reported relative to the most intense peak and are given in parentheses using the following abbreviations: w = weak, m = medium, s = strong. UV-vis spectra were recorded with a Cary 5000 UV-vis-NIR spectrophotometer in toluene and THF. Elemental analyses were performed by Midwest Microlabs, LLC.

*Synthesis of [$Cl_2Ti(\mu\text{-}NIm^{Dipp})]_2$ (**1**).* A 20 mL scintillation vial containing a small magnetic stir bar was loaded with sodium metal (0.050 g, 2.15 mmol) and mercury (0.432 g, 2.15 mmol), forming an amalgam. To it, C_7H_8 (12 mL) was added followed by ($Im^{Dipp}N$)$TiCl_3$ (1.00 g, 1.80 mmol), giving a heterogeneous bright orange mixture. After stirring over 2 d at room temperature, the solution formed an intense, dark blue color with an insoluble precipitate (NaCl). The product mixture was filtered through Celite (2 × 3 cm) supported on a medium porosity glass frit. The filtrate was concentrated under vacuum to 5 mL and layered with pentane (3 mL). Storage at -35 °C for 12 h provided diamond-shaped, deep blue crystals of **1**·1.5C_7H_8. Yield: 838 mg, 79%. (Note: Compound **1**·1.5C_7H_8 is highly soluble in ethereal solvents such as THF and Et_2O, as well as in aromatic solvents such as C_7H_8 and C_6H_6, while insoluble in non-polar solvents like hexanes and pentane.) ^{1}H NMR (25 °C, 400 MHz, C_6D_6): δ 0.99 (d, 24H, J_{HH} = 6.7 Hz, *Me*$_2$CH), 1.53 (d, 24H, J_{HH} = 6.5 Hz, *Me*$_2$CH), 3.02 (sept, 8H, J_{HH} = 6.4 Hz, Me$_2$C*H*), 5.91 (s, 4H, Imid *H*C=C*H*), 7.18 (d, 8H, J_{HH} = 9.4 Hz, *aryl*), 7.32 (t, 4H, J_{HH} = 7.7 Hz, *aryl*). ^{13}C{^{1}H} NMR (25 °C, 101 MHz, C_6D_6): δ 23.93 (*Me*$_2$CH), 25.77 (*Me*$_2$CH), 28.98 (Me$_2$*C*H), 118.71 (Imid H*C*=*C*H), 124.95 (*aryl*), 131.39 (*aryl*), 132.83 (*aryl*), 147.2 (*aryl*), 162.48 (*C*N$_3$). UV-vis (C_7H_8, 0.249 mM, 25 °C, nm, ε = L·mol^{-1}·cm^{-1}): 585 (ε = 699), 690 (ε = 547). Anal. Calcd. For $C_{54}H_{72}Cl_4N_6Ti_2$·1.5C_7H_8: C, 65.72; H, 7.23; N, 7.08. Found: C, 65.42; H, 7.34; N, 7.41.

*Synthesis of [(μ-N-η^6-Im^{Dipp})Ti]$_2$ (**2**).* A solution of **1**·1.5C_7H_8 (1.00 g, 0.85 mmol) in C_7H_8 (30 mL) was prepared inside a 100 mL round bottom flask loaded with a large magnetic stir bar. The dark blue solution was chilled to -35 °C prior to addition of DMPE (1μL, 0.90 mg, 5.99 μmol) and KC_8 (0.481 g, 3.56 mmol). The heterogeneous mixture was stirred at -35 °C for 5 – 7 d. During this time, the reaction mixture turned very dark in color and was subsequently filtered through Celite (2 × 3 cm) supported on a medium porosity glass frit. The filter cake was washed with THF (3 × 10 mL). The filtrate was dried under vacuum yielding a fine powder, which was redissolved in THF/Et_2O (1:8 mL) and stored at -35 °C. After 12 h, dark brown crystalline solid was isolated. Yield: 480 mg, 63%. (Note: Alternatively, the filter cake can be washed with DME (3 × 10 mL) and crystals can be grown from a DME/hexanes solution (10:1 mL). Compound **2** is highly soluble in THF and DME, partially soluble in Et_2O and aromatic solvents, such as C_7H_8 and C_6H_6, and insoluble in non-polar solvents such as hexanes and pentane.) ^{1}H NMR (25 °C, 400 MHz, C_6D_6): δ -39.98, -15.38, -0.62, 0.75, 2.22, 3.91, 4.11, 6.12, 6.28, 25.85. ^{1}H NMR (25 °C, 400 MHz, THF-d_8): δ -39.79, -16.23, -0.75, 0.77, 1.28, 2.13, 2.57, 4.72, 5.90, 6.29, 6.48, 25.36. UV-vis (C_7H_8, 0.258 mM, 25 °C, nm, ε = L·mol^{-1}·cm^{-1}): 232 (ε = 24,654), 293 (ε = 23,594), 384 (ε = 4,534), 616 (ε = 1,870), 823 (ε = 1,572). IR (25 °C, film, cm^{-1}): 659 (s), 671 (m), 718 (m), 722 (m), 755 (m), 765 (s), 800 (m), 808 (m), 859 (s), 876 (w), 885 (w), 905 (w), 929 (s), 949 (w), 989 (m), 1004 (m), 1046 (m), 1056 (m), 1076 (w), 1105 (m), 1118 (m), 1178 (w),1211 (m), 1237 (m), 1254 (w), 1255 (w), 1302 (w), 1315 (w), 1345 (s), 1353 (s), 1357 (m), 1382 (m), 1413 (s), 1435 (m), 1445 (s), 1454 (s), 1460 (m), 1464 (w), 1495 (w), 1504 (m), 1515 (m), 1519 (s), 1524 (s), 1556 (m), 1567 (m), 1587 (m), 2350 (w), 2858 (m), 2924 (w), 2956 (m), 3068 (w), 3136 (w), 3164 (w). IR for **2** + CO reaction product (25 °C, KBr pellet, cm^{-1}): 3630 (w), 3400 (w), 3323 (w), 3172 (w), 3136 (w), 3069 (w), 3029 (w), 2962 (s), 2928 (m), 2868 (m), 2055 (w), 2029 (w), 1632 (s), 1599 (s), 1523 (s), 1470 (s), 1407 (w), 1385 (w), 1362 (m), 1348 (m), 1307 (w), 1257 (w), 1226 (w), 1214 (w), 1181 (w), 1147 (w), 1120 (w), 1106 (m), 1060 (m), 1021 (w), 957 (w), 936 (m), 914 (m), 884 (w), 808 (s), 769 (w), 755 (s), 729 (w), 716 (w), 695 (w), 674 (m), 604 (w), 508 (w), 466 (w), 439 (w), 420 (w). Anal. Calcd. For $C_{54}H_{72}N_6Ti_2$: C, 71.99; H, 8.06; N, 9.33. Found: C, 66.09; H, 7.62; N, 8.40. Repeated combustion analyses performed on several samples failed to give satisfactory results possibly due to the sensitivity of the compound or presence of trace amounts of **3**.

*Synthesis of {[(Et_2O)$_2$K](μ-N-μ-η^6:η^6-Im^{Dipp})Ti}$_2$ (**3**).* A solution of **1**·1.5C_7H_8 (1.00 g, 0.85 mmol) in Et_2O (30 mL) was prepared inside a 100 mL round bottom flask loaded with a large magnetic stir bar. The dark blue solution was chilled to -35 °C prior to addition of KC_8 (710 mg, 5.25 mmol). The heterogeneous mixture was stirred at -35 °C for 12 h, over which time, the solution turned an intense dark brown color. The resulting mixture was filtered through Celite (2 × 3 cm) supported on a medium porosity glass frit. The filtrate was concentrated to 10 mL under vacuum, layered with pentane (2 mL) and stored at -35 °C. After 12 h, dark brown crystalline solid was isolated. Yield: 323 mg, 30%. (Note: Compound **3** is highly soluble in THF and Et_2O, partially soluble in aromatic solvents, such as C_7H_8 and C_6H_6, and insoluble in non-polar solvents such as hexanes and pentane.) UV-vis (THF, 0.094 mM, 25 °C, nm, ε = L·mol^{-1}·cm^{-1}): 212 (ε = 24,858), 242 (ε = 31,400), 300 (ε = 28,561), 616 (ε = 1,964), 885 (ε = 1,081). IR (25 °C, film, cm^{-1}): 659 (s), 690 (m), 762 (s), 778 (w), 789 (w), 801 (m), 808 (w), 847 (m), 860 (m), 875 (m), 922 (m), 932 (w), 976 (m), 994 (m), 1003 (w), 1042 (w), 1058 (m), 1106 (w), 1119 (m), 1179 (w), 1192 (m), 1207 (w), 1229 (m), 1257 (m), 1301 (w), 1344 (s), 1382 (m), 1413 (m), 1434 (w), 1443 (s), 1453 (s), 1460 (m), 1467 (w), 1493 (w), 1503 (m), 1519 (s), 1524 (s), 1555 (s), 1566 (w), 1588 (m), 2345 (w), 2361 (w), 2857 (m), 2921 (w), 2949 (m), 3059 (w), 3131 (w), 3163 (w). IR for **3** + CO reaction product (25 °C, KBr pellet, cm^{-1}): 3399 (w), 3324 (w), 3131 (w), 3067 (w), 2961 (w), 2904 (s), 2925 (w), 2904 (w), 2868 (s), 2207 (w), 2137 (w), 2005 (w), 1629 (s), 1577 (w), 1534 (m), 1473 (s), 1400 (w), 1384 (w), 1351 (s), 1298 (w), 1252 (w), 1226 (w), 1108 (s), 1060 (w), 962 (m), 915 (w), 838 (w), 809 (m), 769 (w), 753 (m), 716 (w), 663 (w), 605 (w). Anal. Calcd. for $C_{54}H_{72}K_2N_6Ti_2$·4Et_2O: C, 65.91; H, 8.85; N, 6.59. Anal. Calcd. For $C_{54}H_{72}K_2N_6Ti_2$·2Et_2O: C, 66.05; H, 8.23; N, 7.45. Found: C, 65.78; H, 8.38; N, 7.70.

*Synthesis of [(Im^{Dipp}N)(η^8-COT)Ti](μ-η^2:η^3-COT)[Ti(η^4-COT)(^{Dipp}NIm)] (**4**).* A 20 mL scintillation vial containing a small magnetic stir bar was loaded with **2** (200 mg, 0.22 mmol) and toluene (8 mL). To the dark brown suspension, COT (74.3 μL, 69.4 mg, 0.66 mmol) was added. Upon addition, the reaction immediately gives way to a homogeneous, dark red solution. Stirring of the mixture at room temperature for 4 h results in the formation of a dark brown coloring. The resulting solution was concentrated to 3 mL under vacuum, layered with hexanes (2 mL), and stored at -35 °C. After 2 - 3 d, crystalline dark plates of **4**·2C_7H_8 were isolated. Yield: 227 mg, 73%. (Note: **4**·2C_7H_8 is highly soluble in THF, partially soluble in Et_2O and aromatic solvents, such as C_7H_8 and C_6H_6, and insoluble in non-polar solvents such as hexanes and pentane.) ^{1}H NMR (25 °C, 400 MHz, C_6D_6): δ 1.19, 1.54, 2.97, 3.22, 5.50, 5.64, 5.76, 7.26. ^{1}H NMR (25 °C, 400 MHz, tol-d_8): δ 1.17, 1.50, 3.20, 5.32, 5.80, 7.23, 7.33. ^{1}H NMR (0 °C, 400 MHz, tol-d_8): δ 1.17, 1.26, 1.58, 3.24, 4.92, 5.52, 5.84, 7.21, 7.37. ^{1}H NMR (-20 °C, 400 MHz, tol-d_8): δ 1.16, 1.27, 1.59 3.25, 4.96, 5.54, 5.81, 7.19, 7.38. ^{1}H NMR (-50 °C, 400 MHz, tol-d_8): δ 1.17, 1.28, 1.60, 3.26, 5.03, 5.56, 5.76, 7.17, 7.38. UV-vis (C_7H_8, 0.070 mM, 25 °C, nm, ε = L·mol^{-1}·cm^{-1}): 286 (ε = 21,836), 322 (ε = 26,969), 430 (ε = 6,242). Anal. Calcd. for $C_{78}H_{96}N_6Ti_2$·2C_7H_8: C, 79.06; H, 8.08; N, 6.01. Anal. Calcd. for $C_{78}H_{96}N_6Ti_2$: C, 77.21; H, 7.97; N, 6.93. Found: C, 63.79; H, 6.99; N, 6.34. Combustion analyses failed to give satisfactory results possibly due to the high sensitivity of the compound or poor combustion properties.

*Synthesis of (Im^{Dipp}N)Ti(η^8-COT)(THF) (**5**)*. **Method A:** Orange-yellow crystalline plates of **5**·0.375C_6H_{14}·0.125THF are obtained upon dissolving **4** into THF followed by layering with hexanes in a 4:1 ratio and storing at -35 °C for 12 h. **Method B:** Addition of COT (46.9 µL, 43.3 mg, 0.42 mmol) to dark brown toluene (6 mL) suspensions of **2** (150 mg, 0.17 mmol) resulted in instant formation of a homogeneous solution accompanied by a color change to dark red. The reaction mixture was stirred at room temperature for 12 h, after which time the solution adopts a dark brown-yellow coloration. The resulting solution was dried under vacuum yielding a fine brown-orange powder, which was redissolved in THF/hexanes (4:1 mL) and stored at -35 °C. After 2 - 3 d, crystalline orange plates of **5**·0.375C_6H_{14}·0.125THF were isolated in 76% yield (84 mg). ^{1}H NMR (25 °C, 400 MHz, C_6D_6): δ 1.18, 1.54, 2.97, 3.21, 5.43, 5.64, 5.76, 7.26. UV-vis (THF, 0.021 mM, 25 °C, nm, ε = L·mol^{-1}·cm^{-1}): 220 (ε = 164,974), 244 (ε = 108,062), 260 (ε = 96,343), 320 (ε = 57,500). Anal. Calcd. for $C_{35}H_{44}N_3Ti_1$·0.375C_6H_{14}·1.125THF: C, 75.06; H, 8.79; N, 6.29. Anal. Calcd. for $C_{35}H_{44}N_3Ti_1$: C, 74.80; H, 8.00; N, 7.58. Found: C, 54.03; H, 6.09; N, 6.30. Combustion analyses failed to give satisfactory results possibly due to the high sensitivity of the compound or poor combustion properties.

Synthesis of [(Im^{Dipp}N)(η^4-COT)Ti(μ-η^4:η^5-COT)K(THF)(μ-η^6:η^4-COT)Ti(NIm^{Dipp})(μ-η^4:η^4-COT)K(THF)$_2$]$_n$ (**6**). A 20 mL scintillation vial containing a small magnetic stir bar was loaded with **3** (200 mg, 0.16 mmol) and toluene (8 mL). To the dark brown suspension, COT (70.6 µL, 65.3 mg, 0.63 mmol) was added. Instant formation of a homogeneous solution was accompanied by a color change to dark red and eventually to dark brown. The reaction mixture stirred for 2 h before forming a layer of an oily, dark material. The residue was solubilized by addition of THF (1 mL), and the mixture was stirred for an additional 2 h. The resulting solution was dried under vacuum yielding a dark powder, which was redissolved in THF (4 mL) layered with hexanes (3 mL) and stored at -35 °C. After 2 – 3 d, crystalline dark blocks of **6**·0.7THF·0.15C_6H_{14} were isolated. Yield: 193 mg, 73%. (Note: The crystalline product is highly soluble in ethereal solvents such as THF and Et_2O and insoluble in aromatic solvents, like C_7H_8 and C_6H_6, and non-polar solvents such as hexanes and pentane.) ^{1}H NMR (25 °C, 400 MHz, C_6D_6/THF-d_8): δ 1.12 (d, 24H, J_{HH} = 6.5 Hz, *Me*$_2$CH), 1.46 (d, 24H, *Me*$_2$CH), 1.51 (m, THF), 3.33 (sept, 8H, J_{HH} = 6.4 Hz, Me$_2$C*H*), 3.53 (m, THF), 5.39 (s, 32H, C_8H_8), 6.11 (s, 4H, Imid *H*C=C*H*), 7.22 (d, 8H, J_{HH} = 7.7 Hz, *aryl*), 7.28 (d, 4H, J_{HH} = 7.7 Hz, *aryl*). ^{13}C{^{1}H} NMR (25 °C, 101 MHz, C_6D_6/THF-d_8): δ 23.14 (*Me*$_2$CH), 25.89 (*Me*$_2$CH), 28.94 (Me$_2$*C*H), 114.56 (Imid *C*=*C*), 124.13 (*aryl*), 129.02 (*aryl*), 136.20 (*aryl*), 140.00 (*aryl*), 147.35 (*C*N$_3$), resonances assignable to the COT ligands were not observed. UV-vis (THF, 0.030 mM, 25 °C, nm, ε = L·mol^{-1}·cm^{-1}): 218 (ε = 84,425), 358 (ε = 35,343), 507 (ε = 7,132), 720 (ε = 2,187). Anal. Calcd. for $C_{86}H_{104}K_2N_6Ti_2$·3.7THF·0.15C_6H_{14}: C, 72.91; H, 8.16; N, 5.02. Anal. Calcd. for $C_{86}H_{104}K_2N_6Ti_2$: C, 74.01; H, 7.51; N, 6.02. Found: C, 73.52; H, 8.02; N, 6.63.

*Synthesis of [(Im^{Dipp}N)Ti(=NAd)](μ-NAd)$_2$[Ti(^{Dipp}NIm)(N$_3$Ad)] (**7**).* A 20 mL scintillation vial containing a small magnetic stir bar was loaded with **2** (300 mg, 0.33 mmol) and toluene (12 mL). The dark brown suspension was chilled to -35 °C prior to addition of AdN_3 (236 mg, 1.33 mmol). Upon addition, immediate gas evolution was accompanied by a color change to dark red. The reaction mixture was stirred at -35 °C for 12 h. The resulting solution was concentrated to 3 mL under vacuum, layered with hexanes (2 mL) and stored at -35 °C. After 3 – 4 d, crystalline, red-orange blocks of **7**·3C_7H_8 were isolated. Yield: 317 mg, 53%. (Note: Attempts to isolate pure samples of **7**·3C_7H_8 are frustrated by the persistent presence of small amounts of **8-tol**. Compound **7**·3C_7H_8 is highly soluble in ethereal solvents, such as THF, DME and Et_2O, and aromatic solvents, like C_7H_8 and C_6H_6. It is also moderately soluble in non-polar solvents such as hexanes and pentanes.) ^{1}H NMR (25 °C, 400 MHz, C_6D_6): δ 1.04-1.06 (6H, *Ad*), 1.22-1.23 (24H, overlapping *Me*$_2$CH and *Ad*), 1.37-1.39 (18H, overlapping *Me*$_2$CH and *Ad*), 1.51-1.52 (12H, overlapping *Me*$_2$CH and *Ad*), 1.59 (24H, overlapping *Me*$_2$CH and *Ad*), 1.87 (18H, *Ad*), 2.15 (6H, *Ad*), 3.18 (sept, 4H, Me$_2$C*H*), 3.75 (sept, 4H, Me$_2$C*H*), 5.80 (s, 2H, Imid *H*C=C*H*), 5.91 (s, 2H, Imid *H*C=C*H*), 7.00-7.27 (12H, *aryl*). Due to severe peak overlap, discrimination of adamantyl C*H* and C*H*$_2$ resonances is not possible and is denoted generally as *Ad*. ^{13}C{^{1}H} NMR (25 °C, 101 MHz, C_6D_6, ppm): δ 24.47 (*Me*$_2$CH), 24.67 (br, *Ad*), 25.46 (*Me*$_2$CH), 29.01 (two overlapping Me$_2$*C*H), 30.26 (*Ad*), 31.32 (*Ad*), 35.82 (*Me*$_2$CH), 36.80 (*Me*$_2$CH), 37.81 (*Ad*), 42.29 (br, *Ad* accounting for 3 resonances), 46.36 (*Ad*), 48.94 (*Ad*), 67.02 (N-*Ad*), 68.00 (N-*Ad*), 114.23 (Imid H*C*=*C*H), 114.42 (Imid H*C*=*C*H), 123.70 (*aryl*), 124.02 (*aryl*), 128.83 (*aryl*), 129.69 (*aryl*), 135.53 (*aryl*), 135.75 (*aryl*), 137.71 (*aryl*), 142.44 (*aryl*), 147.44 (*C*N$_3$), 148.40 (*C*N$_3$), one N-*Ad* resonance not observed. IR (25 °C, film, cm^{-1}): 679 (w), 757 (m), 769 (w), 793 (w), 800 (w), 810 (w), 862 (w), 878 (w), 888 (w), 907 (w), 1003 (w), 1026 (w), 1060 (w), 1070 (w), 1095 (w), 1133 (w), 1179 (w), 1223 (w), 1245 (w), 1255 (w), 1297 (w), 1351 (w), 1361 (w), 1391 (w), 1454 (m), 1460 (m), 1565 (s), 1582 (m), 1600 (s), 1618 (m), 1629 (m), 2088 (m), 2846 (m), 2869 (m), 2904 (s), 2960 (s).

*Synthesis of [(Im^{Dipp}N)Ti(NHAd)](μ-NAd)$_2$[Ti(C$_6$H$_4$Me)(^{Dipp}NIm)] (**8-tol**)*. A 20 mL scintillation vial containing a small magnetic stir bar was loaded with **2** (300 mg, 0.33 mmol) and toluene (12 mL). To the resulting dark brown suspension, AdN_3 (177 mg, 1.00 mmol) was added. Upon addition, immediate gas evolution was accompanied by a color change to red-yellow. The reaction mixture was stirred at room temperature for 1 h. The resulting solution was concentrated to 5 mL under vacuum, layered with pentane (3 mL) and stored at -35 °C. After 3 – 4 d, crystalline, red-yellow blocks were isolated. Yield: 340 mg, 73%. (Note: **8-tol** is soluble in THF and aromatic solvents, like C_7H_8 and C_6H_6, while partially soluble in Et_2O and non-polar solvents such as hexanes and pentane.) ^{1}H NMR (25 °C, 400 MHz, C_6D_6, ppm): δ 1.17-1.18 (36H, 2 overlapping d, overlapping *Me*$_2$CH), 1.20-1.21 (18H, overlapping Ad-C*H*$_2$ and Ad-C*H*), 1.24-1.27 (32H, overlapping Ad-C*H*$_2$ and *Me*$_2$CH), 1.39-1.44 (12H, overlapping Ad-C*H*$_2$), 1.47-1.50 (18H, overlapping Ad-C*H*$_2$ and Ad-C*H*), 1.51-1.53 (28H, overlapping Ad-C*H*$_2$ and *Me*$_2$CH), 1.71-1.74 (6H, Ad-C*H*$_2$), 1.78-1.81 (18H, overlapping Ad-C*H*$_2$ and *Me*$_2$CH), 1.98 (6H, Ad-C*H*$_2$), 2.02 (6H, Ad-C*H*$_2$), 2.19 (3H, Ad-C*H*), 2.25 (3H, Ad-C*H*), 2.26 (s, 3H, C$_6$H$_4$*Me*, *p*-isomer), 2.47 (s, 3H, C$_6$H$_4$*Me*, *m*-isomer), 3.29 (2 overlapping sept, 16H, overlapping Me$_2$C*H*), 5.68 (s, 4H, Imid *H*C=C*H*), 5.82 (d, 4H, Imid *H*C=C*H*), 6.64 (s, 1H, N*H*), 6.65 (s, 1H, N*H*), 7.05 (m, 1H, C$_6$*H*$_4$Me, *m*-isomer), 7.10-7.12 (m, 9H, overlapping *aryl m*-isomer and *p*-isomer), 7.18-7.20 (8H, overlapping *aryl*), 7.23 (d, 2H, C$_6$*H*$_4$Me, *p*-isomer), 7.25-7.27 (4H, overlapping *aryl*), 7.97 (d, 1H, C$_6$*H*$_4$Me, *m*-isomer), 8.04 (s, 1H, C$_6$*H*$_4$Me, *m*-isomer), 8.13 (d, 2H, C$_6$*H*$_4$Me, *p*-isomer). Signals corresponding to specific stereoisomers are assigned where possible. ^{13}C{^{1}H} NMR (25 °C, 101 MHz, C_6D_6, ppm): δ 21.93 (C$_6$H$_4$*Me*, *p*-isomer), 22.37 (C$_6$H$_4$*Me*, *m*-isomer), 23.60-25.27 (7 signals, overlapping Ad-*C*H$_2$ and *Me*$_2$CH), 28.92 (Ad-*C*H$_2$), 28.99 (Me$_2$*C*H), 29.02 (Me$_2$*C*H), 30.88 (Ad-*C*H$_2$), 30.94 (*Me*$_2$CH), 30.97 (*Me*$_2$CH), 36.49 (Ad-*C*H), 37.36 (Ad-*C*H), 37.39 (Ad-*C*H), 47.60 (Ad-*C*H), 47.64 (Ad-*C*H), 47.76 (Ad-*C*H), 47.84 (Ad-*C*H), 57.60 (HN-*C*$_{Ad}$), 57.66 (HN-*C*$_{Ad}$), 69.52 (N-*C*$_{Ad}$, imido), 69.55 (N-*C*$_{Ad}$, imido), 114.75 (Imid H*C*=*C*H), 115.64 (Imid *HC*=*C*H), 115.68 (Imid H*C*=*C*H), 124.21 (*C*$_6$H$_4$Me, *m*-isomer), 124.58 (*aryl*), 125.21 (*aryl*), 125.70 (*aryl*), 126.39 (*aryl*), 128.57 (*C*$_6$H$_4$Me), 129.34 (*C*$_6$H$_4$Me), 129.37 (*aryl*), 129.42 (*aryl*), 130.09 (*C*$_6$H$_4$Me, *p*-isomer), 133.54 (aryl), 134.22 (aryl), 134.89 (*aryl*), 135.78 (*aryl*), 135.81 (*aryl*), 136.46 (*aryl*), 136.49 (*aryl*), 137.88 (*C*$_6$H$_4$Me, *m*-isomer), 138.48 (*C*$_6$H$_4$Me, *p*-isomer), 140.28 (*aryl*), 140.44 (*aryl*), 147.52 (*C*N$_3$), 147.60 (*C*N$_3$), 186.00 (*meta* Ti-*C*$_6$H$_4$Me, *m*-isomer), 188.88 (*para* Ti-*C*$_6$H$_4$Me, *p*-isomer). UV-vis (C_7H_8, a.u., 25 °C, nm): 284, 342, 433, 571. IR (25 °C, film, cm^{-1}): 647 (m), 656 (m), 702 (m), 726 (m), 736 (m), 759 (s), 769 (m), 787 (m), 802 (m), 811 (m), 880 (m), 890 (m), 907 (m), 932 (m), 947 (m), 994 (m), 1009 (m), 1070 (m), 1094 (m), 1118 (m), 1137 (m), 1167 (m), 1180 (m), 1226

(m), 1256 (m), 1299 (m), 1331 (m), 1348 (s), 1362 (m), 1384 (m), 1398 (m), 1455 (s), 1544 (s), 1567 (s), 1599 (s), 1634 (w), 1656 (w), 1699 (w), 1703 (w), 1725 (w), 1810 (w), 1938 (w), 1985 (w), 2653 (w), 2674 (w), 2845 (s), 2902 (s), 2962 (s), 3066 (w), 3107 (w), 3132 (w), 3272 (w). Anal. Calcd. for $C_{91}H_{125}N_9Ti_2$: C, 75.86; H, 8.74; N, 8.75. Anal. Calcd. for $C_{91}H_{125}N_9Ti_2 \cdot 0.5C_5H_{12}$: C, 75.94; H, 8.98; N, 8.57. Found: C, 75.95; H, 8.75; N, 8.17.

Synthesis of [(Im^{Dipp}N)Ti(NHAd)](μ-NAd)$_2$[Ti(C$_6$H$_5$)(^{Dipp}*NIm)] (**8-C$_6$H$_5$**).* A 20 mL scintillation vial containing a small magnetic stir bar was loaded with **2** (150 mg, 0.33 mmol) and C_6H_6 (12 mL). To the resulting dark brown suspension, AdN_3 (177 mg, 1.00 mmol) was added. Upon addition, immediate gas evolution was accompanied by a color change to red-yellow. The reaction mixture stirred at room temperature for 1 h. The resulting solution was concentrated to 5 mL under vacuum, layered with pentane (3 mL) and stored at room temperature. After 2 d, crystalline, yellow blocks of **8-C$_6$H$_5$**$\cdot 0.5C_6H_6 \cdot 0.75C_5H_{12}$ were isolated. Yield: 152 mg, 60%. (Note: Compound **8-C$_6$H$_5$**$\cdot 0.5C_6H_6 \cdot 0.75C_5H_{12}$ is soluble in THF and aromatic solvents like C_7H_8 and C_6H_6, while partially soluble in non-polar solvents such as hexanes and pentane.) ^{1}H NMR (25 °C, 400 MHz, C_6D_6): δ 1.17-1.20 (m, 24H, overlapping *Me*$_2$CH), 1.22 (6H, Ad-C*H*$_2$), 1.24 (d, 12H, J_{HH} = 6.8 Hz, *Me*$_2$CH), 1.40-1.43 (6H, Ad-C*H*$_2$), 1.48 (12H, Ad-C*H*$_2$), 1.51 (d, 12H, J_{HH} = 6.8 Hz, *Me*$_2$CH), 1.72-1.74 (3H, Ad-C*H*), 1.79 (9H, overlapping Ad-C*H*$_2$ and Ad-C*H*), 1.99 (6H, Ad-C*H*$_2$), 2.22 (3H, Ad-C*H*), 3.30 (m, 8H, overlapping Me$_2$C*H*), 5.68 (s, 2H, Imid *H*C=C*H*), 5.83 (s, 2H, Imid *H*C=C*H*), 6.65 (s, 1H, N*H*), 7.10-7.12 (4H, *aryl*), 7.18 (4H, *aryl*), 7.20-7.25 (m, 4H, *aryl*), 7.27-7.33 (m, 3H, overlapping *m*- and *p*-C$_6$*H*$_5$), 8.20 (d, 2H, *o*-C$_6$*H*$_5$). ^{13}C{^{1}H} NMR (25 °C, 101 MHz, C_6D_6): δ 23.58 (*Me*$_2$CH), 24.19 (*Me*$_2$CH), 24.87 (*Me*$_2$CH), 25.26 (*Me*$_2$CH), 28.92 (Me$_2$CH), 29.01 (Me$_2$*C*H), 30.87 (Ad-*C*H$_2$), 30.94 (Ad-*C*H), 36.48 (Ad-*C*H$_2$), 37.35 (Ad-*C*H), 47.60 (Ad-*C*H$_2$), 47.81 (Ad-*C*H$_2$), 57.65 (HN-*C*$_{Ad}$), 69.55 (N-*C*$_{Ad}$, imido), 114.75 (Imid H*C*=*C*H), 115.66 (Imid H*C*=*C*H), 124.21 (*aryl*), 124.58 (*aryl*), 125.53 (*m*-*C*$_6$H$_5$), 125.69 (*p*-*C*$_6$H$_5$), 129.44 (*aryl*), 130.11 (*aryl*), 135.74 (*aryl*), 136.44 (*aryl*), 137.80 (*o*-*C*$_6$H$_5$), 140.31 (*C*N$_3$), 140.46 (*C*N$_3$), 147.57 (*aryl*), 188.89 (*C*$_6$H$_5$). UV-vis (C_7H_8, 0.063 mM, 25 °C, nm, ε = L·mol^{-1}·cm^{-1}): 283 (ε = 17.542), 340 (ε = 22,346), 433 (ε = 16,286), 574 (ε = 95).

*Synthesis of [(Im^{Dipp}N)Ti(NCPh$_3$)(κ^1-DME)]$_2$(μ-η^2:η^2-N$_2$) (**9**).* A 20 mL scintillation vial containing a small magnetic stir bar was loaded with **2** (300 mg, 0.33 mmol) and toluene (12 mL). The resulting dark brown suspension was chilled to -35 °C prior to addition of Ph_3CN_3 (285 mg, 1.00 mmol). Upon addition, immediate gas evolution was accompanied by a color change to dark red-yellow. The reaction mixture was stirred at -35 °C for 6 h. The resulting solution was dried under vacuum, yielding an orange-red fine powder, which was redissolved in DME (6 mL) and stored at -35 °C. After 2 d, diamond-shaped, dark orange crystals were isolated. Yield: 22 mg, 4%. UV-vis (C_7H_8, a.u., 25 °C, nm): 356, 435, 550. IR (25 °C, film, cm^{-1}): 635 (s), 650 (m), 694 (m), 701 (s), 729 (m), 742 (w), 755 (m), 771 (w), 801 (w), 873 (m), 888 (w), 903 (w), 915 (w), 937 (w), 1028 (m), 1060 (w), 1078 (w), 1118 (w), 1151 (w), 1173 (m), 1198 (m), 1223 (w), 1256 (w), 1297 (w), 1342 (w), 1359 (w), 1390 (m), 1442 (m), 1454 (m), 1463 (m), 1503 (w), 1519 (w), 1537 (w), 1556 (w), 1563 (m), 1579 (m), 1610 (m), 2864 (w), 2923 (w), 2960 (w), 3052 (w), 3583 (w). (Note: Compound **9** is partially soluble in ethereal solvents such as THF, DME, and Et_2O, aromatic solvents, like C_7H_8 and C_6H_6, and non-polar solvents such as hexanes and pentane.)

*Synthesis of [K(18-crown-6)(THF)$_2$][{[(Im^{Dipp}N)Ti(NAd)](μ-NAd)$_2$K[Ti(NIm^{Dipp})]} (**10**).* A 20 mL scintillation vial containing a small magnetic stir bar was loaded with **3** (300 mg, 0.24 mmol) and toluene (12 mL). To the resulting dark brown suspension, AdN_3 (167 mg, 0.96 mmol) was added followed by 18-crown-6 (124.3 mg, 0.48 mmol). Upon addition, immediate gas evolution was accompanied by a color change to dark red. The reaction mixture stirred at room temperature for 12 h. The resulting solution was dried under vacuum yielding an orange-red fine powder, which was redissolved in THF (4 mL) and layered with pentane (2 mL) and stored at -35 °C. After 5 – 7 d, crystalline, pink-orange blocks of **10**·THF were isolated. Yield: 309 mg, 69%. (Note: Compound **10**·THF is highly soluble in THF and aromatic solvents, like C_7H_8 and C_6H_6, while insoluble in non-polar solvents such as hexanes and pentane.) ^{1}H NMR (25 °C, 400 MHz, C_6D_6, ppm): δ 1.30-1.32 (m, 18H, overlapping *Me*$_2$CH and Ad-C*H*$_2$), 1.39-1.41 (m, 18H, overlapping *Me*$_2$CH and Ad-C*H*$_2$), 1.42 (br s, 12H, coordinated and co-crystallized THF), 1.60 – 1.64 (br s, 12H, Ad-C*H*$_2$), 1.69 (br s,12H, *Me*$_2$CH), 1.78 (m, 15H, overlapping *Me*$_2$CH and Ad-C*H*), 1.91 (br s, 6H, Ad-C*H*$_2$), 1.97 (br s, 3H, Ad-C*H*), 2.22 (br s, 6H, Ad-C*H*$_2$), 2.31 (br s, 3H, Ad-C*H*), 3.24 (s, 24H, $C_{12}H_{24}O_6$), 3.57 (br s, 12H, coordinated and co-crystallized THF), 3.75 (br s, 4H, Me$_2$C*H*), 3.96 (br s, 4H, Me$_2$C*H*), 5.96 (s, 2H, Imid *H*C=C*H*), 6.04 (s, 2H, Imid *H*C=C*H*), 7.26 – 7.28 (m, 12H, *aryl*). ^{13}C{^{1}H} NMR (25 °C, 101 MHz, C_6D_6, ppm): δ 24.58 (*Ad*), 24.86 (*Me*$_2$CH), 24.97 (*Ad*), 25.72 (*Ad*), 25.84 (THF), 29.00 (overlapping Me$_2$C*H*), 31.15 (*Me*$_2$CH), 31.55 (*Ad*), 37.29 (*Me*$_2$CH), 38.20 (*Ad*), 45.99 (*Me*$_2$CH), 49.18 (*Ad*), 66.35 (N-*C*$_{Ad}$), 67.84 (THF), 70.19 (*C*$_{12}$H$_{24}$O$_6$), 114.19 (Imid H*C*=*C*H), 114.39 (Imid H*C*=*C*H), 123.59 (*aryl*), 124.24 (*aryl*), 128.18 (*aryl* overlap with C_6D_6), 128.28 (*aryl* overlap with C_6D_6) 137.70 (*aryl*), 147.91(*C*N$_3$), 148.92 (*C*N$_3$), one N-*C*$_{Ad}$ and one aryl resonance not observed. Due to severe peak overlap, discrimination of adamantyl C*H* and C*H*$_2$ resonances is not possible and is denoted generally as *Ad*. UV-vis (C_7H_8, 0.231 mM, 25 °C, nm, ε = L·mol^{-1}·cm^{-1}): 295 (ε = 13,720), 340 (ε = 13,806), 445 (ε = 1,908), 550 nm (ε = 128). Anal. Calcd. for $C_{104}H_{157}K_2N_9O_8Ti_2 \cdot$1THF: C, 68.00; H, 8.72; N, 6.61. Anal. Calcd. for $C_{104}H_{157}K_2N_9O_8Ti_2$: C, 68.06; H, 8.62; N, 6.87. Found: C, 65.86; H, 8.69; N, 6.61. Combustion analyses failed to give satisfactory results possibly due to the high sensitivity of the compound or poor combustion properties.

X-ray Structure Solution and Refinement. Data for **3** and **7**$\cdot 3C_7H_8$ were collected on a Bruker D8 Quest 3-axis diffractometer equipped with a Photon II CMOS detector using a graphite monochromator with a Mo Kα sealed-tube X-ray source (α = 0.71073 Å), while data for **1**$\cdot 1.5C_7H_8$, **2**-*Pccn*, **2**-*P*$\bar{1}$, **4**$\cdot 2C_7H_8$, **5**$\cdot 0.375C_6H_{14} \cdot 0.125C_7H_8$, **6**$\cdot$0.7THF$\cdot 0.15C_6H_{14}$, **8-tol**, **8-C$_6H_5$**$\cdot 0.5C_6H_6 \cdot 0.75C_5H_{12}$, **9**, and **10**·THF were collected on a dual source Bruker D8 Venture 4-axis diffractometer equipped with a PHOTON II CPAD detector and a IμS Mo Kα X-ray source (α = 0.71073 Å) fitted with a HELIOS MX monochromator. Crystals were mounted on a Mitigen Kapton loop, coated in NVH oil, and maintained at 100(2) K under a flow of nitrogen gas during data collection. Data collection and cell parameter determination were conducted using the SMART program.[87] Integration of the data and final cell parameter refinements were performed using SAINT[88] software with data absorption correction implemented through SADABS.[89] Structures were solved using intrinsic phasing methods and difference Fourier techniques. All hydrogen atom positions were idealized and rode on the atom of attachment. Structure solution, refinement, graphics, and creation of publication materials were performed using SHELXTL[90] or the Olex[91] crystallographic package. Relevant crystallographic data is presented in Table S1 and complete crystallographic data for complexes **1**$\cdot 1.5C_7H_8$, **2**-*Pccn*, **2**-*P*$\bar{1}$, **3**, **5**$\cdot 0.375C_6H_{14} \cdot 0.125C_7H_8$, **6**$\cdot$0.7THF$\cdot 0.15C_6H_{14}$, **8-tol**, **8-C$_6H_5$**$\cdot 0.5C_6H_6 \cdot 0.75C_5H_{12}$, **9**, and **10**·THF has been deposited in the Cambridge Crystallographic Data Center under the following CCDC deposit numbers: 2175031 (**1**$\cdot 1.5C_7H_8$), 2175029 (**2**-*Pccn*), 2175024 (**2**-*P*$\bar{1}$), 2175023 (**3**), 2175026 (**5**$\cdot 0.375C_6H_{14} \cdot 0.125C_7H_8$), 2165032 (**6**$\cdot$0.7THF$\cdot 0.15C_6H_{14}$), 2175025 (**8-tol**), 2175027 (**-C$_6$H$_5$**$\cdot 0.5C_6H_6 \cdot 0.75C_5H_{12}$), 2175028 (**9**), 2175030 (**10**·THF).

In **1**$\cdot 1.5C_7H_8$, one toluene molecule exhibits positional disorder and was modeled over two positions with SADI restrains

applied to all ring carbon-carbon bonds (C55 to C61). Similarly, the remaining half toluene molecule was modeled over two positions with half-occupancies and DFIX restrains were applied to all carbon-carbon bonds (1.4 C63-C65, 1.51 C62-C63). Moreover, reflections -4 6 8, -13 5 1, and 7 5 5 were omitted as outliers. Positional disorder of an isopropyl substituent in **2**-*Pccn* and **3** was addressed by modeling the methyl carbons (C12, C13 in **2a**; C19, C20 in **3**) in two orientations in which occupancies were determined through data refinement. In **6**·0.7THF·0.15C_6H_{14}, the K1-coordinated THF molecule (O1, C52-C55) displays severe positional disorder and was modeled over two positions with occupancies assigned based on data refinement. Moreover, residual electron density corresponds to one THF (O4, C99-C012) and one-half hexanes (C103-C105) equivalents which were assigned fixed occupancies of 0.7 and 0.3 respectively with 2 hexanes C-C bond distances restrained by DFIX to 1.53 Å. For complex **7**·3C_7H_8, carbon atoms C23-C25, C28-C30 belonging to the adamantyl substituent in fragment Ti1-N3Ad, Ti2 coordinated N_3Ad unit, and a co-crystallized toluene molecule (C109-C115) exhibit positional disorder; in all cases, such disorder was modeled by splitting the electron density over two orientations with occupancies determined through data refinement. Within the Im-^{Dipp}N$^-$ ligands, methyl carbons C59, C60, C72, C73, C93 and C94 were also found to be disordered over two orientations. In addition, AFIX restrains were used over the co-crystallized toluene molecules (C95-C101, C102-108) to help model positional disorder and an ISOR 0.01 restrain was used on C31A. Despite best efforts, the wR2 value could not be improved beyond 27.3%, thus its data is only presented to demonstrate connectivity and general structural features. In **8-tol**, reflections 0 1 5, 0 3 3, 0 1 3, and 0 2 4 were omitted as outliers. In addition, disordered isopropyl substituents were modeled by splitting the electron density over two orientations with occupancies determined through data refinement, and carbon-carbon bond lengths C62-C63A, C62-C63B, C62-C64A, C62-C64B, C89-C90A, C89-C90B, C89-C91A, and C89-C91B were fixed to 1.53 Å using a DFIX constrain. In **8-C_6H_5**·0.5C_6H_6·0.75C_5H_{12}, residual electron density corresponding to overlapping, non-coordinated benzene (C91-C96) and pentane (C97-C101) molecules was modeled assigning half occupancy to each solvent molecule; while half a pentane equivalent also found in the asymmetric unit was assigned an occupancy of 0.5. THF molecules coordinated to the potassium atom K2 within the cation in complex **10**·THF display severe positional disorder over two positions and were modeled as such. Additionally, atoms C12, C14, C17, C18 and C20, belonging to the adamantyl substituent coordinated to bridging nitrogen atom N2, exhibit positional disorder and are better represented by modeling over two positions with occupancies determined through data refinement and bond lengths restricted by the use of DFIX 1.53 Å. Residual electron density corresponding to highly disordered, co-crystallized pentane molecules could not be fully modeled and instead the density was removed using the PLATON/SQUEEZE algorithm.[92] Residual electron density corresponding to highly disordered toluene/pentane in compound **8-tol**, and THF in **10**·THF could not be accurately modeled and was removed using the PLATON/SQUEEZE algorithm.[92]

Magnetic Measurements.

The magnetic susceptibility measurements for complexes **2**, **3**, and **4**·2C_7H_8 were obtained using a Quantum Design SQUID magnetometer MPMS-XL7 operating between 1.8 and 300 K (**2**) and 2.0 and 300 K (**3** and **4**·2C_7H_8). DC measurements were performed on a crushed polycrystalline sample of 32.0 mg for **2**, which was subjected to fields of -7 to 7T. The sample was restrained with silicon grease and wrapped in a polyethylene membrane under an inert atmosphere. The magnetization data was collected at 100 K to check for ferromagnetic impurities. For complexes **3**, and **4**·2C_7H_8 DC measurements using 1T fields were performed on crystalline samples of 19.7 mg and 15.2 mg, respectively. The samples were sandwiched between eicosane layers (~1.5 mm/each) inside glass NMR tubes, which were flame sealed under nitrogen. Diamagnetic corrections were applied for the sample holder and inherent diamagnetic contributions were estimated with the use of Pascals constants and used to correct effective magnetic moment calculations.

ASSOCIATED CONTENT

Supporting Information.

NMR, UV-vis, and IR spectral data, SQUID magnetometry data, and solid-state molecular structures of **1**·1.5C_7H_8, **2**-*Pccn*, **2**-*P*$\bar{1}$, **3**, **4**·2C_7H_8, **5**·0.375C_6H_{14}·0.125C_7H_8, **6**·0.7THF·0.15C_6H_{14}, **7**·3C_7H_8, **8-tol**, **8-C_6H_5**·0.5C_6H_6·0.75C_5H_{12}, **9**, and **10**·THF.

AUTHOR INFORMATION

Corresponding Author

*E-mail: asfortier@utep.edu

ORCID

Skye Fortier: 0000-0002-0502-5229
Muralee Murugesu: 0000-0002-5123-374X
Alejandra Gómez-Torres: 0000-0002-2663-0807
Niki Mavragani: 0000-0003-0069-3233
Alejandro Metta-Magaña: 0000-0001-9993-8485

Notes

The authors declare no competing financial interest.

ACKNOWLEDGMENT

S.F is grateful to the Welch Foundation (AH-1922-20200401) for financial support of this work. S.F. is an Alfred P. Sloan research fellow and is thankful for their support. We also wish to acknowledge the NSF-MRI program for providing funding for the purchase of an X-ray diffractometer and SQUID magnetometer (CHE-1827875; DMR-2018067). N.M. and M.M. are grateful for the support from the University of Ottawa, the Natural Sciences and Engineering Research Council of Canada, and the Canadian Foundation for Innovation.

REFERENCES

1. Powers, T. M.; Betley, T. A., Testing the Polynuclear Hypothesis: Multielectron Reduction of Small Molecules by Triiron Reaction Sites. *J. Am. Chem. Soc.* **2013**, *135*, 12289-12296.
2. Zhao, Q. L.; Betley, T. A., Synthesis and Redox Properties of Triiron Complexes Featuring Strong Fe-Fe Interactions. *Angew. Chem. Int. Ed.* **2011**, *50*, 709-712.
3. Pivrikas, A.; Sariciftci, N. S.; Juska, G.; Osterbacka, R., A review of charge transport and recombination in polymer/fullerene organic solar cells. *Prog. Photovolt.* **2007**, *15*, 677-696.
4. Jiang, Z. P.; Zhao, Y. M.; Lu, X.; Xie, J., Fullerenes for rechargeable battery applications: Recent developments and future perspectives. *J. Energy Chem.* **2021**, *55*, 70-79.
5. Fertig, A. A.; Brennessel, W. W.; McKone, J. R.; Matson, E. M., Concerted Multiproton-Multielectron Transfer for the Reduction of O_2 to H_2O with a Polyoxovanadate Cluster. *J. Am. Chem. Soc.* **2021**, *143*, 15756-15768.
6. Toniolo, D.; Scopelliti, R.; Zivkovic, I.; Mazzanti, M., Assembly of High-Spin [Fe-3] Clusters by Ligand-Based Multielectron Reduction. *J. Am. Chem. Soc.* **2020**, *142*, 7301-7305.
7. Ferreira, R. B.; Murray, L. J., Cyclophanes as Platforms for Reactive Multimetallic Complexes. *Accounts Chem Res* **2019**, *52*, 447-455.
8. Ohsawa, Y.; Saji, T., Electrochemical Detection of $C60^{6-}$ at Low-Temperature. *J. Chem. Soc. Chem. Comm.* **1992**, 781-782.

9. Xie, Q. S.; Perezcordero, E.; Echegoyen, L., Electrochemical Detection of C_{60}^{6-} and C_{70}^{6-} - Enhanced Stability of Fullerides in Solution. *J. Am. Chem. Soc.* **1992**, *114*, 3978-3980.
10. Hoffman, B. M.; Lukoyanov, D.; Yang, Z. Y.; Dean, D. R.; Seefeldt, L. C., Mechanism of Nitrogen Fixation by Nitrogenase: The Next Stage. *Chem. Rev.* **2014**, *114*, 4041-4062.
11. Singh, D.; Buratto, W. R.; Torres, J. F.; Murray, L. J., Activation of Dinitrogen by Polynuclear Metal Complexes. *Chem. Rev.* **2020**, *120*, 5517-5581.
12. Eaton, M. C.; Catalano, V. J.; Shearer, J.; Murray, L. J., Dinitrogen Insertion and Cleavage by a Metal-Metal Bonded Tricobalt(I) Cluster. *J. Am. Chem. Soc.* **2021**, *143*, 5649-5653.
13. Nair, A. K.; Harisomayajula, N. V. S.; Tsai, Y. C., The lengths of the metal-to-metal quintuple bonds and reactivity thereof. *Inorg. Chim. Acta.* **2015**, *424*, 51-62.
14. Ni, C. B.; Ellis, B. D.; Long, G. J.; Power, P. P., Reactions of Ar'CrCrAr' with N_2O or N_3(1-Ad): complete cleavage of the Cr-Cr quintuple interaction. *Chem. Commun.* **2009**, 2332-2334.
15. Noor, A.; Glatz, G.; Muller, R.; Kaupp, M.; Demeshko, S.; Kempe, R., Carboalumination of a chromium-chromium quintuple bond. *Nat. Chem.* **2009**, *1*, 322-325.
16. Beaumier, E. P.; Pearce, A. J.; See, X. Y.; Tonks, I. A., Modern applications of low-valent early transition metals in synthesis and catalysis. *Nat. Rev. Chem.* **2019**, *3*, 15-34.
17. Davis-Gilbert, Z. W.; Tonks, I. A., Titanium redox catalysis: insights and applications of an earth-abundant base metal. *Dalton Trans.* **2017**, *46*, 11522-11528.
18. Manssen, M.; Schafer, L. L., Titanium catalysis for the synthesis of fine chemicals - development and trends. *Chem. Soc. Rev.* **2020**, *49*, 6947-6994.
19. Fortier, S.; Gomez-Torres, A., Redox chemistry of discrete low-valent titanium complexes and low-valent titanium synthons. *Chem. Commun.* **2021**, *57*, 10292-10316.
20. Aguilar-Calderón, J. R.; Murillo, J.; Gomez-Torres, A.; Saucedo, C.; Jordan, A.; Metta-Magaña, A. J.; Pink, M.; Fortier, S., Redox Character and Small Molecule Reactivity of a Masked Titanium(II) Synthon. *Organometallics* **2020**, *39*, 295-311.
21. Gómez-Torres, A.; Aguilar-Calderón, J. R.; Encerrado-Manriquez, A. M.; Pink, M.; Metta-Magaña, A. J.; Lee, W.-Y.; Fortier, S., Titanium-Mediated Catalytic Hydrogenation of Monocyclic and Polycyclic Arenes. *Chem. Eur. J.* **2020**, *26*, 2803-2807.
22. Gómez-Torres, A.; Aguilar-Calderón, J. R.; Saucedo, C.; Jordan, A.; Metta-Magaña, A.; Pinter, B.; Fortier, S., Reversible oxidative-addition and reductive-elimination of thiophene from a titanium complex and its thermally-induced hydrodesulphurization chemistry. *Chem. Commun.* **2020**, *56*, 1545-1548.
23. Kilpatrick, A. F. R.; Cloke, F. G. N., Reductive deoxygenation of CO_2 by a bimetallic titanium bis(pentalene) complex. *Chem. Commun.* **2014**, *50*, 2769-2771.
24. Kilpatrick, A. F. R.; Green, J. C.; Cloke, F. G. N., The Reductive Activation of CO_2 Across a Ti=Ti Double Bond: Synthetic, Structural, and Mechanistic Studies. *Organometallics* **2015**, *34*, 4816-4829.
25. Kilpatrick, A. F. R.; Green, J. C.; Cloke, F. G. N., Reactivity of a Dititanium Bis(pentalene) Complex toward Heteroallenes and Main-Group Element-Element Bonds. *Organometallics* **2017**, *36*, 352-362.
26. Kilpatrick, A. F. R.; Green, J. C.; Cloke, F. G. N.; Tsoureas, N., Bis(pentalene)di-titanium: a bent double-sandwich complex with a very short Ti-Ti bond. *Chem. Commun.* **2013**, *49*, 9434-9436.
27. Tsoureas, N.; Green, J. C.; Cloke, F. G. N., C-H and H-H activation at a di-titanium centre. *Chem. Commun.* **2017**, *53*, 13117-13120.
28. Hagadorn, J. R.; Arnold, J., Titanium(II), -(III), and -(IV) complexes supported by benzamidinate ligands. *Organometallics* **1998**, *17*, 1355-1368.
29. Shima, T.; Hu, S. W.; Luo, G.; Kang, X. H.; Luo, Y.; Hou, Z. M., Dinitrogen Cleavage and Hydrogenation by a Trinuclear Titanium Polyhydride Complex. *Science* **2013**, *340*, 1549-1552.
30. Cummins, C. C.; Schaller, C. P.; Van Duyne, G. D.; Wolczanski, P. T.; Chan, A. W. E.; Hoffmann, R., Tri-tert-butylsilyl)imido complexes of titanium: benzene carbon-hydrogen activation and structure of $[(^tBu_3SiNH)Ti]_2(\mu\text{-}NSi^tBu_3)_2$. *J. Am. Chem. Soc.* **1991**, *113*, 2985-2994.
31. Castillo, M.; Barreda, O.; Maity, A. K.; Barraza, B.; Lu, J.; Metta-Magaña, A. J.; Fortier, S., Advances in guanidine ligand design: synthesis of a strongly electron-donating, imidazolin-2-iminato functionalized guanidinate and its properties on iron. *J. Coord. Chem.* **2016**, *69*, 2003-2014.
32. Franz, D.; Irran, E.; Inoue, S., Synthesis, characterization and reactivity of an imidazolin-2-iminato aluminium dihydride. *Dalton Trans.* **2014**, *43*, 4451-4461.
33. Alvarez, S., A cartography of the van der Waals territories. *Dalton Trans.* **2013,** *42*, 8617-8636.
34. Jilek, R. E.; Jang, M.; Smolensky, E. D.; Britton, J. D.; Ellis, J. E., Structurally Distinct Homoleptic Anthracene Complexes, $[M(C_{14}H_{10})_3]^{2-}$, M = Titanium, Zirconium, Hafnium: Tris(arene) Complexes for a Triad of Transition Metals. *Angew. Chem. Int. Ed.* **2008**, *47*, 8692-8695.
35. Aguilar-Calderón, J. R.; Metta-Magaña, A. J.; Noll, B.; Fortier, S., $C(sp^3)$−H Oxidative Addition and Transfer Hydrogenation Chemistry of a Titanium(II) Synthon: Mimicry of Late-Metal Type Reactivity. *Angew. Chem. Int. Ed.* **2016**, *55*, 14101-14105.
36. Buchwald, S. L.; Nielsen, R. B., Group 4 metal complexes of benzynes, cycloalkynes, acyclic alkynes, and alkenes. *Chem. Rev.* **1988**, *88*, 1047-1058.
37. Ozerov, O. V.; Patrick, B. O.; Ladipo, F. T., Highly Regioselective [2 + 2 + 2] Cycloaddition of Terminal Alkynes Catalyzed by η^6-Arene Complexes of Titanium Supported by Dimethylsilyl-Bridged p-tert-Butyl Calix[4]arene Ligand. *J. Am. Chem. Soc.* **2000**, *122*, 6423-6431.
38. Hill, J. E.; Balaich, G.; Fanwick, P. E.; Rothwell, I. P., The chemistry of titanacyclopentadiene rings supported by 2,6-diphenylphenoxide ligation: stoichiometric and catalytic reactivity. *Organometallics* **1993**, *12*, 2911-2924.
39. Reiner, B. R.; Tonks, I. A., Group 4 Diarylmetallocenes as Bespoke Aryne Precursors for Titanium-Catalyzed [2 + 2 + 2] Cycloaddition of Arynes and Alkynes. *Inorg. Chem.* **2019**, *58*, 10508-10515.
40. Ozerov, O. V.; Ladipo, F. T.; Patrick, B. O., Highly Regioselective Alkyne Cyclotrimerization Catalyzed by Titanium Complexes Supported by Proximally Bridged p-tert-Butylcalix[4]arene Ligands. *J. Am. Chem. Soc.* **1999**, *121*, 7941-7942.
41. Cohen, S. A.; Bercaw, J. E., Titanacycles derived from reductive coupling of nitriles, alkynes, acetaldehyde, and carbon dioxide with bis(pentamethylcyclopentadienyl)(ethylene)titanium(II). *Organometallics* **1985**, *4*, 1006-1014.
42. Fortier, S.; Gomez-Torres, A.; Saucedo, C., Arene Complexes of the Group 4 Metals. In *Comprehensive Organometallic Chemistry IV*, Elsevier: **2021**.
43. Brauer, D. J.; Krüger, C., The structure of bis(cyclooctatetraene)(tetrahydrofuran)zirconium. *J. Organomet. Chem.* **1972,** *42*, 129-137.
44. Highcock, W. J.; Mills, R. M.; Spencer, J. L.; Woodward, P., The relative stability of cyclo-octatetraene complexes of zirconium(II) and zirconium(IV); X-ray crystal structure of [Zr(η-C_3H_5)(η-C_3Me_5)-(1–4-η-C_8H_8)]. *J. Chem. Soc., Chem. Commun.* **1982**, 128-129.
45. Highcock, W. J.; Mills, R. M.; Spencer, J. L.; Woodward, P., Allyl derivatives of (cyclo-octatetraene)(η-pentamethylcyclopentadienyl)-zirconium: X-ray crystal structure of [Zr(η-C_5Me_5)(1–4-η-C_8H_8)(η-C_3H_5)]. *J. Chem. Soc., Dalton Trans.* **1986**, 829-833.
46. Berno, P.; Floriani, C.; Chiesi-Villa, A.; Rizzoli, C., Bis(cyclooctatetraene) derivatives of zirconium(IV) and hafnium(IV): syntheses and Lewis base adducts. Crystal structures of [Zr(η^8-C_8H_8)(η^4-C_8H_8)], [Hf{η^8-$C_8H_6(SiMe_3)_2$}(η^4-$C_8H_6(SiMe_3)_2$}], [Zr(η^8-C_8H_8)(η^4-C_8H_8)(NH_3)] and [Zr(η^8-C_8H_8)(η^4-C_8H_8)(CNBut)]. *J. Chem. Soc., Dalton Trans.* **1991**, 3085-3091.

47. Rogers, D. M.; Wilson, S. R.; Girolami, G. S., Bis(cyclooctatetraenyl)zirconium: x-ray crystal structure and solution and solid-state NMR spectra. *Organometallics* **1991,** *10*, 2419-2424.
48. Sinnema, P. J.; Meetsma, A.; Teuben, J. H., Competitive CH activation in (pentamethylcyclopentadienyl)(cyclooctatetraene)alkylzirconium compounds $Cp^*Zr(COT)R$. Selective formation of fulvene or cyclooctatrienyne ligands. Molecular structure of $Cp^*Zr(\mu\text{-}\eta^8\text{:}\ \eta^2\text{-}C_8H_6)ZrCp^*(\eta^4\text{-}C_8H_8)$, a dinuclear zwitterionic zirconium complex with a bridging cyclooctatrienyne ligand. *Organometallics* **1993,** *12*, 184-189.
49. Cloke, F. G. N.; Green, J. C.; Hitchcock, P. B.; Joseph, S. C. P.; Mountford, P.; Kaltsoyannis, N.; McCamley, A., Molecular and electronic structures of bis[1,4-bis(trimethylsilyl)cyclooctatetraene] sandwich complexes of titanium and zirconium. *J. Chem. Soc., Dalton Trans.* **1994**, 2867-2874.
50. Dietrich, H. S., M., Zur Kristallstruktur von Bis(cyclooctatetraen)titan. *Angew. Chem.* **1969,** *81*.
51. Dierks, H.; Dietrich, H., Die Kristallstruktur von Tris-cyclooctatetraen-dititan. *Acta Crystallographica Section B* **1968,** *24*, 58-62.
52. Schwartz, J.; Sadler, J. E., Ring 'flipping' in bis(cyclo-octatetraene)titanium(II); an organometallic intramolecular redox reaction which involves only the geometrical deformation of organic ligands. *J. Chem. Soc., Chem. Commun.* **1973**, 172-173.
53. Cloke, F. G. N.; Green, J. C.; Hazari, N.; Hitchcock, P. B.; Mountford, P.; Nixon, J. F.; Wilson, D. J., Reactions of ^{t}BuC⁝P with Cyclooctatetraene-Supported Titanium Imido Complexes. *Organometallics* **2006,** *25*, 3688-3700.
54. Mukhopadhyay, T. K.; Flores, M.; Feller, R. K.; Scott, B. L.; Taylor, R. D.; Paz-Pasternak, M.; Henson, N. J.; Rein, F. N.; Smythe, N. C.; Trovitch, R. J.; Gordon, J. C., A New Spin on Cyclooctatetraene (COT) Redox Activity: Low-Spin Iron(I) Complexes That Exhibit Antiferromagnetic Coupling to a Singly Reduced η4-COT Ligand. *Organometallics* **2014**, *33*, 7101-7112.
55. Panda, T. K.; Trambitas, A. G.; Bannenberg, T.; Hrib, C. G.; Randoll, S.; Jones, P. G.; Tamm, M., Imidazolin-2-iminato Complexes of Rare Earth Metals with Very Short Metal−Nitrogen Bonds: Experimental and Theoretical Studies. *Inorg. Chem.* **2009**, *48*, 5462-5472.
56. Glockner, A.; Bannenberg, T.; Daniliuc, C. G.; Jones, P. G.; Tamm, M., From a Cycloheptatrienylzirconium Allyl Complex to a Cycloheptatrienylzirconium Imidazolin-2-iminato "Pogo Stick" Complex with Imido-Type Reactivity. *Inorg. Chem.* **2012**, *51*, 4368-4378.
57. Calderazzo, F.; Ferri, I.; Pampaloni, G.; Englert, U.; Green, M. L. H., Synthesis of $[Ti(h^6\text{-}1,3,5\text{-}C_6H_3{}^iPr_3)][BAr_4]$ (Ar = C_6H_5, p-C_6H_4F, 3,5-$C_6H_3(CF_3)_2$), the first titanium(I) derivatives. *Organometallics* **1997**, *16*, 3100-3101.
58. Geoffrey, F.; Cloke, N., Titanium Complexes in Oxidation States Zero and Below. In *Comprehensive Organometallic Chemistry II*, Abel, E. W.; Stone, F. G. A.; Wilkinson, G., Eds. Elsevier: Oxford, **1995**, 213-219.
59. Chirik, P. J.; Bouwkamp, M. W., Complexes of Titanium in Oxidation States 0 to II. In *Comprehensive Organometallic Chemistry III*, Mingos, D. M. P.; Crabtree, R. H., Eds. Elsevier: Oxford, **2007**, 243-279.
60. Heins, S. P.; Zhang, B.; MacMillan, S. N.; Cundari, T. R.; Wolczanski, P. T., Oxidative Additions to Ti(IV) in $[(dadi)^{4-}]Ti^{IV}$(THF) Involve Carbon–Carbon Bond Formation and Redox-Noninnocent Behavior. *Organometallics* **2019**, *38*, 1502-1515.
61. Zanotti-Gerosa, A.; Solari, E.; Giannini, L.; Floriani, C.; Re, N.; Chiesi-Villa, A.; Rizzoli, C., Titanium-carbon functionalities on an oxo surface defined by a calix [4] arene moiety and its redox chemistry. *Inorg. Chim. Acta* **1998**, *270*, 298-311.
62. Yang, H.-T.; Zhou, S.; Chang, F.-S.; Chen, C.-R.; Gau, H.-M., Synthesis, Structures, and Characterizations of $[ArTi(O^iPr)_3]_2$ and Efficient Room-Temperature Aryl−Aryl Coupling of Aryl Bromides with $[ArTi(O^iPr)_3]_2$ Catalyzed by the Economic $Pd(OAc)_2/PCy_3$ System. *Organometallics* **2009**, *28*, 5715-5721.
63. Zeinstra, J. D.; Teuben, J. H.; Jellinek, F., Structure of μ-dinitrogenbis[*p*-tolyldicyclopentadienyl-titanium(III)], $[(C_5H_5)_2Ti(p\text{-}CH_3C_6H_4)]_2N_2$. *J. Organomet. Chem.* **1979**, *170*, 39-50.
64. Armstrong, D. R.; García-Álvarez, J.; Graham, D. V.; Honeyman, G. W.; Hevia, E.; Kennedy, A. R.; Mulvey, R. E., Synthetic and Structural Insights into the Zincation of Toluene: Direct Synergic Ring Metallation versus Indirect Nonsynergic Lateral Metallation. *Eur. J. Chem.* **2009**, *15*, 3800-3807.
65. Brand, S.; Elsen, H.; Langer, J.; Grams, S.; Harder, S., Calcium-Catalyzed Arene C−H Bond Activation by Low-Valent All. *Angew. Chem. Int. Ed.* **2019**, *58*, 15496-15503.
66. Cummins, C. C.; Baxter, S. M.; Wolczanski, P. T., Methane and benzene activation via transient $(^tBu_3SiNH)_2Zr{:}NSi^tBu_3$. *J. Am. Chem. Soc.* **1988**, *110*, 8731-8733.
67. Walsh, P. J.; Hollander, F. J.; Bergman, R. G., Monomeric and dimeric zirconocene imido compounds: synthesis, structure, and reactivity. *Organometallics* **1993**, *12*, 3705-3723.
68. Bennett, J. L.; Wolczanski, P. T., Selectivities in Hydrocarbon Activation: Kinetic and Thermodynamic Investigations of Reversible 1,2-RH-Elimination from $(silox)_2(^tBu_3SiNH)TiR$ (silox = $^tBu_3SiO$). *J. Am. Chem. Soc.* **1997**, *119*, 10696-10719.
69. Duncan, A. P.; Bergman, R. G., Selective transformations of organic compounds by imidozirconocene complexes. *Chem. Rec.* **2002**, *2*, 431-445.
70. Lee, S. Y.; Bergman, R. G., Reactions of an Imidozirconocene Complex with Cyclopentadienylmetal Carbonyl Complexes: C-H Activation versus Oxygen Atom Abstraction. *J. Am. Chem. Soc.* **1995**, *117*, 5877-5878.
71. Hoyt, H. M.; Michael, F. E.; Bergman, R. G., C−H Bond Activation of Hydrocarbons by an Imidozirconocene Complex. *J. Am. Chem. Soc.* **2004**, *126*, 1018-1019.
72. Walsh, P. J.; Hollander, F. J.; Bergman, R. G., Generation, alkyne cycloaddition, arene carbon-hydrogen activation, nitrogen-hydrogen activation and dative ligand trapping reactions of the first monomeric imidozirconocene ($Cp_2Zr{:}NR$) complexes. *J. Am. Chem. Soc.* **1988**, *110*, 8729-8731.
73. Wigley, D. E., Organoimido Complexes of the Transition Metals. In *Progress in Inorganic Chemistry* **1994**, 239-482.
74. Hanna, T. E.; Bernskoetter, W. H.; Bouwkamp, M. W.; Lobkovsky, E.; Chirik, P. J., Bis(cyclopentadienyl) Titanium Dinitrogen Chemistry: Synthesis and Characterization of a Side-on Bound Haptomer. *Organometallics* **2007**, *26*, 2431-2438.
75. Semproni, S. P.; Milsmann, C.; Chirik, P. J., Side-on Dinitrogen Complexes of Titanocenes with Disubstituted Cyclopentadienyl Ligands: Synthesis, Structure, and Spectroscopic Characterization. *Organometallics* **2012**, *31*, 3672-3682.
76. Duchateau, R.; Gambarotta, S.; Beydoun, N.; Bensimon, C., Side-on versus end-on coordination of dinitrogen to titanium(II) and mixed-valence titanium(I)/titanium(II) amido complexes. *J. Am. Chem. Soc.* **1991**, *113*, 8986-8988.
77. Hirotsu, M.; Fontaine, P. P.; Zavalij, P. Y.; Sita, L. R., Extreme N⁝N Bond Elongation and Facile N-Atom Functionalization Reactions within Two Structurally Versatile New Families of Group 4 Bimetallic "Side-on-Bridged" Dinitrogen Complexes for Zirconium and Hafnium. *J. Am. Chem. Soc.* **2007**, *129*, 12690-12692.
78. Pool, J. A.; Lobkovsky, E.; Chirik, P. J., Hydrogenation and cleavage of dinitrogen to ammonia with a zirconium complex. *Nature* **2004**, *427*, 527-530.
79. Pool, J. A.; Lobkovsky, E.; Chirik, P. J., Cyclopentadienyl Substituent Effects on Reductive Elimination Reactions in Group 4 Metallocenes: Kinetics, Mechanism, and Application to Dinitrogen Activation. *J. Am. Chem. Soc.* **2003**, *125*, 2241-2251.
80. Berno, P.; Hao, S.; Minhas, R.; Gambarotta, S., Dinitrogen Fixation versus Metal-Metal Bond Formation in the Chemistry of Vanadium(II) Amidinates. *J. Am. Chem. Soc.* **1994**, *116*, 7417-7418.
81. Campazzi, E.; Solari, E.; Floriani, C.; Scopelliti, R., The fixation and reduction of dinitrogen using lanthanides: praseodymium

and neodymium meso-octaethylporphyrinogen–dinitrogen complexes. *Chem. Commun.* **1998**, 2603-2604.
82. Hao, S. K.; Feghali, K.; Gambarotta, S., Preparation and characterization of a diamagnetic and dinuclear titanium(III) formamidinate complex. Evidence for the existence of a Ti-Ti bond? *Inorg. Chem.* **1997**, *36*, 1745-1748.
83. Duncan Lyngdoh, R. H.; Schaefer, H. F.; King, R. B., Metal–Metal (MM) Bond Distances and Bond Orders in Binuclear Metal Complexes of the First Row Transition Metals Titanium Through Zinc. *Chem. Rev.* **2018**, *118*, 11626-11706.
84. Shoken, D.; Sharma, M.; Botoshansky, M.; Tamm, M.; Eisen, M. S., Mono(imidazolin-2-iminato) Titanium Complexes for Ethylene Polymerization at Low Amounts of Methylaluminoxane. *J. Am. Chem. Soc.* **2013**, *135*, 12592-12595.
85. Yadav, M.; Metta-Magana, A. J.; Fortier, S., Intra- and intermolecular interception of a photochemically generated terminal uranium nitride. *Chem. Sci.* **2020**, *11*, 2381-2387.
86. Gokel, G. W.; Cram, D. J.; Liotta, C. L.; Harris, H. P.; Cook, F. L., Preparation and Purification of 18-Crown-6. *J. Org. Chem.* **1974**, *39*, 2445-2446.
87. SMART APEX II. Bruker AXS Inc. Madison, WI.
88. SAINT Software User's Guide. Bruker AXS Inc. Madison, WI.
89. Blessing, R., An empirical correction for absorption anisotropy. *Acta Crystallogr. A* **1995,** *51*, 33-38.
90. Sheldrick, G. M., SHELXTL. *Bruker AXS Inc. Madison, WI*.
91. Dolomanov, O. V.; Bourhis, L. J.; Gildea, R. J.; Howard, J. A. K.; Puschmann, H., OLEX2: a complete structure solution, refinement and analysis program. *J. Appl. Crystallogr.* **2009**, *42*, 339-341.
92. Spek, A., PLATON SQUEEZE: a tool for the calculation of the disordered solvent contribution to the calculated structure factors. *Acta Crystallogr. C* **2015**, *71*, 9-18.